

Supplementary Data

SUPPLEMENTARY TABLE:

Supplementary table 1: Mass, assignment, and intensity of peaks in positive ion mode, the different classes observed are PE, Galcer, DAG, PC and Cer with different cationization. Cer-H₂O, DAG-H₂O and PA are reported in red as they can have multiple origins.

Supplementary table 2: Mass, assignment and intensity of peaks in negative ion mode, the different classes observed are PE, ST, PI and Galcer as deprotonated species, and SM-H-CH₂. PA are reported in red as they can have multiple origins.

Supplementary table 3: Intensity and coefficient of variation from lipids peak in 4 successive tissue sections sorted by lipids class and cationization

SUPPLEMENTARY FIGURE:

Supplementary figure 1: Positive ion mode spectra of lipid standards on rat brain tissue implanted with AgNP and MALDI images extracted from one of the major cationization.

Supplementary figure 2: Negative ion mode spectra of lipid standards on rat brain tissue implanted with AgNP and MALDI images extracted from deprotonated ion.

Supplementary figure 3: MALDI images in negative ion mode from deposited lipids on a rat brain section, the image has been extracted for the m/z 227.2006 corresponding to Mystic Acid(14:0)-H. This image shows that this peak can be produced by several lipid standards

Supplementary figure 4: MALDI images extracted for all lipids species identified in positive and negative ion mode. In positive ion mode all images shown are produced from silver cationization while in negative ion mode they are produced from M-H peak except for SM in which M-H-CH₂ was used.

Supplementary figure 5: MALDI average mass spectrum from a serial rat section, acquired in negative ion mode on a MALDI-LTQ-Orbitrap-XL with silver nanoparticles matrices.

Supplementary figure 6: Distribution of ceramides by mass imaging of a rat at brain section level -2.0 mm re:Bregma in positive ion mode and comparison of microscope image before and after Implantation.

Supplementary figure 7: Distribution of ceramides by mass imaging at level -3.2 mm re:Bregma in positive ion mode in a rat brain section, resolution 100,000 at 400 u.

Supplementary table 1: Mass, assignment, and intensity of peaks in positive ion mode, the different classes observed are PE, Galcer, DAG, PC and Cer with different cationization. Cer-H₂O, DAG-H₂O and PA are reported in red as they can have multiple origins.

Assignments	Theoretical m/z	m/z _{obs}	Counts	Error (ppm)
Cer-H ₂ O 16:0/d18:1 +Ag	626.4066	626.4067	4.0E+03	0.1
Cer 16:0/d18:1+Ag	644.4166	644.4179	1.3E+03	2.0
Cer-H ₂ O 18:1/d18:1 or 18:0/d18:2 +Ag	652.4223	652.4232	6.5E+04	1.4
Cer-H ₂ O 18:0/d18:1 +Ag	654.4379	654.4388	2.1E+05	1.4
DAG-H ₂ O 32a:1 +Ag	655.3856	655.3864	1.3E+04	1.3
DAG-H ₂ O 32a:0 +Ag	657.4012	657.4021	9.5E+04	1.3
Cer 18:1/d18:1 or 18:0/d18:2+Ag	670.4323	670.4335	6.5E+04	1.8
Cer 18:0/d18:1+Ag	672.4479	672.4490	1.6E+05	1.6
DAG 32a:0+Ag	675.4112	675.4127	4.6E+03	2.2
DAG-H ₂ O 34a:2 +Ag	681.4012	681.4022	4.0E+04	1.5
Cer-H ₂ O 20:0/d18:1 +Ag	682.4692	682.4703	4.5E+04	1.6
DAG-H ₂ O 34a:1 +Ag	683.4169	683.4177	7.3E+05	1.3
DAG-H ₂ O 34a:0 +Ag	685.4325	685.4332	8.8E+04	1.0
DAG 34a:2+Ag	699.4112	699.4128	1.3E+03	2.2
Cer 20:0/d18:1+Ag	700.4792	700.4807	2.5E+04	2.1
DAG 34a:1+Ag	701.4269	701.4284	4.4E+04	2.1
DAG-H ₂ O 36a:5 +Ag	703.3856	703.3866	1.8E+03	1.4
DAG-H ₂ O 36a:4 +Ag	705.4012	705.4025	9.4E+04	1.8
Cholesterol+3Ag	707.0696	707.0718	5.5E+04	3.1
DAG-H ₂ O 36a:3 +Ag	707.4169	707.4179	2.6E+04	1.5
DAG-H ₂ O 36a:2 +Ag	709.4325	709.4337	1.2E+05	1.7
Cer-H ₂ O 22:0/d18:1 +Ag	710.5005	710.5016	8.2E+03	1.4
DAG-H ₂ O 36a:1 +Ag	711.4482	711.4492	3.4E+05	1.5
DAG-H ₂ O 38p:6 +Ag	713.4063	713.4076	3.8E+04	1.9
DAG-H ₂ O 36a:0 +Ag	713.4638	713.4646	1.4E+05	1.0
DAG-H ₂ O 38e:6 +Ag	715.4219	715.4231	3.3E+04	1.7
DAG-H ₂ O 38p:4 +Ag	717.4376	717.4389	1.1E+05	1.8

Assignments	Theoretical m/z	m/z _{obs}	Counts	Error (ppm)
DAG-H ₂ O 38e:4+Ag	719.4532	719.4540	1.0E+04	1.0
Cer-H ₂ O 23:1/d 18:1+Ag	722.5005	722.5016	2.9E+03	1.5
Galcer 16:0/d 18:1+Na	722.5541	722.5544	1.7E+03	0.4
DAG 36a:4+Ag	723.4112	723.4126	3.3E+03	1.9
DAG-H ₂ O 38a:7+Ag	727.3856	727.3867	1.4E+03	1.5
DAG 36a:2+Ag	727.4425	727.4441	9.9E+03	2.1
DAG-H ₂ O 38a:6+Ag	729.4012	729.4026	1.2E+05	1.9
DAG 36a:1+Ag	729.4582	729.4597	4.8E+04	2.1
DAG-H ₂ O 38a:5+Ag	731.4169	731.4181	8.8E+04	1.7
CE 16:0	731.4896	731.4905	6.4E+02	1.1
DAG-H ₂ O 38a:4+Ag	733.4325	733.4338	4.2E+05	1.7
Cer-H ₂ O 24:1/d 18:2+Ag	734.5005	734.5018	2.0E+04	1.7
DAG-H ₂ O 38a:3+Ag	735.4482	735.4492	9.6E+04	1.4
Cer-H ₂ O 24:1/d 18:1 or 24:0/d 18:2+Ag	736.5162	736.5175	1.3E+05	1.8
DAG-H ₂ O 38a:2+Ag	737.4638	737.4647	3.1E+04	1.3
Cer-H ₂ O 24:0/d 18:1+Ag	738.5318	738.5330	3.1E+04	1.7
DAG-H ₂ O 38a:1+Ag	739.4795	739.4796	3.6E+04	0.1
DAG-H ₂ O 40p:6+Ag	741.4376	741.4390	1.3E+05	1.9
DAG-H ₂ O 38a:0+Ag	741.4951	741.4960	3.1E+04	1.2
DAG-H ₂ O 40e:6+Ag	743.4532	743.4542	2.1E+04	1.4
DAG 38a:6+Ag	747.4112	747.4130	7.7E+03	2.4
Galcer 18:0/d 18:1+Na	750.5854	750.5870	7.9E+03	2.1
DAG 38a:4+Ag	751.4425	751.4441	6.5E+04	2.1
Cer 24:1/d 18:2+Ag or Cer-H ₂ O 24:1(OH)/d 18:1 +Ag	752.5105	752.5125	5.8E+04	2.6
Cer 24:1/d 18:1+Ag or Cer-H ₂ O 24:0(OH)/d 18:1 +Ag	754.5262	754.5280	1.2E+05	2.3
DAG-H ₂ O 40a:7+Ag	755.4169	755.4181	3.7E+04	1.7
Cer 24:0/d 18:1+Ag	756.5418	756.5443	1.0E+04	3.3

Assignments	Theoretical m/z	m/z _{obs}	Counts	Error (ppm)
PC 32:0a+Na	756.5514	756.5517	1.2E+04	0.4
DAG-H ₂ O 40a:6+Ag	757.4325	757.4336	5.2E+05	1.4
CE 18:1	757.5053	757.5058	1.5E+03	0.7
DAG-H ₂ O 40a:5+Ag	759.4482	759.4491	1.2E+05	1.2
DAG-H ₂ O 40a:4+Ag	761.4638	761.4649	8.6E+04	1.4
DAG-H ₂ O 40a:3+Ag	763.4795	763.4800	3.5E+04	0.7
Galcer 18:0/d18:1+K	766.5594	766.5607	4.4E+03	1.7
PC 32a:0+K	772.5253	772.5251	4.4E+04	-0.3
DAG 40a:6+Ag	775.4425	775.4443	4.6E+04	2.3
PE 34p:1-H+2K	778.4550	778.4565	3.5E+04	1.9
PE 34a:1-H+Na+K	778.4760	778.4776	6.8E+03	2.1
Galcer 20:0/d18:1+Na	778.6167	778.6181	1.7E+03	1.7
CE 20:4	779.4896	779.4902	1.1E+04	0.7
PC 34a:1+Na	782.5670	782.5685	2.1E+04	1.8
PE 36p:4-H+Na+K	784.4654	784.4668	8.5E+02	1.7
PC 34a:0+Na	784.5827	784.5834	4.8E+02	0.9
PE 36e:4-H+Na+K	786.4810	786.4827	5.4E+02	2.1
PE 36p:1-H+Na+K	790.5124	790.5143	2.1E+04	2.5
PE 36p:0-H+Na+K	792.5280	792.5300	6.5E+02	2.5
PE34a:1-H+2K	794.4499	794.4518	3.2E+04	2.4
Galcer 20:0/d18:1+K	794.5907	794.5919	6.7E+02	1.5
Galcer 20:0(OH)/d18:1+Na	794.6117	794.6129	6.3E+02	1.5
PC 34a:2+K	796.5253	796.5258	8.9E+02	0.6
PC 34a:1+K	798.5410	798.5426	7.4E+04	2.0
PE 36p:4-H+2K	800.4393	800.4414	5.1E+03	2.5
PE 36a:4-H+Na+K	800.4603	800.4618	5.4E+02	1.9
PC 34a:0+K	800.5566	800.5576	4.9E+03	1.2

Assignments	Theoretical m/z	m/z _{obs}	Counts	Error (ppm)
PA 38:4-H+2K	801.4233	801.4248	3.3E+04	1.8
CE 22:6	803.4896	803.4905	4.3E+03	1.1
PE 36p:2-H+2K	804.4706	804.4726	4.4E+04	2.5
PE 36a:2-H+Na+K	804.4916	804.4936	2.1E+04	2.5
Galcer 22:1/d18:1 or 22:0/d18:2+Na	804.6324	804.6340	4.6E+02	2.0
Galcer 16:0/d18:1+Ag	806.4695	806.4709	2.4E+03	1.8
PE 36p:1-H+2K	806.4863	806.4883	5.8E+04	2.5
PE 36a:1-H+Na+K	806.5073	806.5093	5.9E+04	2.5
Galcer 22:0/d18:1+Na	806.6480	806.6495	3.1E+03	1.8
PE 38p:6-H+Na+K	808.4654	808.4672	5.3E+03	2.3
PE 36p:0-H+2K	808.5019	808.5037	5.4E+03	2.2
PE 36a:0-H+Na+K	808.5229	808.5238	1.5E+03	1.1
PE 38p:5-H+Na+K	810.4811	810.4826	1.6E+03	1.9
Galcer 20:0(OH)/d18:1+K	810.5856	810.5886	4.8E+02	3.7
PC 36a:1+Na	810.5983	810.5993	1.0E+03	1.2
PE 38p:4-H+Na+K	812.4967	812.4987	1.7E+04	2.4
PE 36a:4-H+2K	816.4343	816.4361	3.1E+03	2.2
PE 36a:2-H+2K	820.4656	820.4676	4.8E+04	2.5
PC 36a:4+K	820.5253	820.5257	2.7E+03	0.4
Galcer 22:1(OH)/d18:1 or 22:0(OH)/d18:2+Na	820.6273	820.6289	4.5E+03	1.9
PE 36a:1-H+2K	822.4812	822.4833	1.6E+05	2.5
Galcer 22:0/d18:1+K	822.6220	822.6237	1.7E+03	2.1
Galcer 22:0(OH)/d18:1+Na	822.6430	822.6449	6.5E+04	2.3
PE 38p:6-H+2K	824.4393	824.4413	2.0E+04	2.4
PE 38a:6-H+Na+K	824.4603	824.4622	9.8E+03	2.3
PE 36a:0-H+2K	824.4969	824.4971	7.6E+03	0.3
PA40:6-H+2K	825.4234	825.4255	7.5E+04	2.6

Assignments	Theoretical m/z	m/z _{obs}	Counts	Error (ppm)
PE 38p:5-H+2K	826.4550	826.4572	8.8E+03	2.7
PE 38a:5-H+Na+K	826.4760	826.4780	2.1E+03	2.5
PC 36a:1+K	826.5723	826.5739	1.1E+04	1.9
PE 38p:4-H+2K	828.4706	828.4729	5.7E+04	2.7
PE 38a:4-H+Na+K	828.4916	828.4936	4.5E+04	2.4
PE 38e:4-H+2K	830.4863	830.4885	4.2E+03	2.7
PE 40a:6+K	830.5097	830.5111	1.3E+04	1.8
Galcer 24:1/d18:2+Na	830.6480	830.6498	5.4E+03	2.1
PA 38:4+Ag	831.4089	831.4098	1.5E+04	1.1
Galcer 18:1/d18:1or 18:0/d18:2+Ag	832.4851	832.4870	3.0E+03	2.2
Galcer 24:1/d18:1or 24:0/d18:2+Na	832.6637	832.6657	6.4E+04	2.4
Galcer 18:0/d18:1+Ag	834.5008	834.5027	5.9E+04	2.3
Galcer 23:1(OH)/d18:1+Na	834.6430	834.6443	4.2E+02	1.6
Galcer 24:0/d18:1+Na	834.6793	834.6812	2.3E+04	2.2
Galcer 22:1(OH)/d18:1+K	836.6012	836.6028	1.6E+03	1.9
Galcer 23:0(OH)/d18:1+Na	836.6586	836.6604	1.6E+04	2.1
Galcer C22:0(OH)/d18:1+K	838.6169	838.6188	4.9E+04	2.2
PE 38a:6-H+2K	840.4343	840.4364	4.1E+04	2.6
PC 32a:0+Ag	840.4667	840.4684	2.2E+04	2.1
PE 38a:5-H+2K	842.4499	842.4521	1.3E+04	2.6
PE 38a:4-H+2K	844.4656	844.4678	1.3E+05	2.7
PA 36:2-H+AgK	845.3647	845.3667	1.8E+04	2.3
PE 34p:1-H+AgK	846.3964	846.3983	2.2E+04	2.3
Galcer 24:1/d18:2+K	846.6220	846.6237	2.1E+03	2.0
Galcer 24:1(OH)/d18:2+Na	846.6430	846.6447	6.2E+03	2.1
PA 36:1-H+AgK	847.3804	847.3822	3.1E+04	2.2
PC 38a:4+K	848.5566	848.5579	6.5E+02	1.5

Assignments	Theoretical m/z	m/z _{obs}	Counts	Error (ppm)
Galcer 24:1/d 18:1 or 24:0/d18:2+K	848.6376	848.6396	4.9E+04	2.3
Galcer 24:1(OH)/d 18:1 or 24:0(OH)/d18:2+Na	848.6586	848.6606	1.1E+05	2.3
PE 40p:7-H+2K	850.4550	850.4566	3.7E+03	1.9
PE 40a:7-H+Na+K	850.4760	850.4781	5.9E+03	2.5
Galcer 18:0(OH)/d 18:1+Ag	850.4957	850.4976	2.5E+04	2.3
Galcer 24:0/d 18:1+K	850.6533	850.6558	1.6E+04	3.0
Galcer 24:0(OH)/d 18:1+Na	850.6743	850.6761	1.6E+05	2.2
PE 40p:6-H+2K	852.4706	852.4731	8.1E+04	2.8
PE 40a:6-H+Na+K	852.4916	852.4937	7.5E+04	2.5
Galcer 23:0(OH)/d 18:1+K	852.6325	852.6343	9.3E+03	2.0
PE 40p:5-H+2K	854.4863	854.4888	8.8E+03	2.9
PA 40:6+Ag	855.4089	855.4106	2.0E+04	2.0
PE 40p:4-H+2K	856.5019	856.5041	1.6E+04	2.5
PE 40a:4-H+Na+K	856.5229	856.5248	5.6E+03	2.2
PE 40e:4-H+2K	858.5176	858.5198	6.3E+02	2.6
Galcer 20:0/d 18:2+Ag	860.5164	860.5181	1.5E+03	2.0
PE 34a:1-H+AgK	862.3913	862.3932	1.0E+04	2.2
Galcer 20:0/d 18:1+Ag	862.5321	862.5339	2.5E+04	2.1
Galcer 24:1(OH)/d 18:2+K	862.6169	862.6183	2.0E+03	1.6
Ag cluster(8)	863.2388	863.2413	8.5E+03	2.9
Galcer 24:1(OH)/d 18:1 or 24:0(OH)/d18:2+K	864.6325	864.6345	7.9E+04	2.3
PE 40a:7-H+2K	866.4499	866.4519	2.4E+04	2.3
PC 34a:1+Ag	866.4824	866.4841	4.2E+04	2.0
Galcer 24:0(OH)/d 18:1+K	866.6482	866.6501	1.2E+05	2.2
PE 36p:4-H+AgK	868.3807	868.3828	3.3E+03	2.4
PE 40a:6-H+2K	868.4656	868.4678	2.2E+05	2.6
PC 34a:0+Ag	868.4980	868.4985	2.5E+03	0.6

Assignments	Theoretical m/z	m/z _{obs}	Counts	Error (ppm)
PA 38:4-H+AgK	869.3647	869.3664	2.0E+04	1.9
PE 36e:4-H+AgK	870.3964	870.3979	7.6E+02	1.7
PE 38a:6+Ag	870.4198	870.4208	7.4E+02	1.3
Galcer 20:4(OH)/d18:1+Ag	870.4644	870.4655	1.4E+04	1.3
PE 40a:5-H+2K	870.4812	870.4820	1.2E+04	1.0
PE 36p:2-H+AgK	872.4120	872.4138	3.2E+04	2.1
PE 40a:4-H+2K	872.4968	872.4989	2.9E+04	2.4
PE 36p:1-H+AgK	874.4277	874.4293	3.8E+04	1.9
Galcer 20:0(OH)/d18:2+Ag	876.5113	876.5130	6.5E+02	2.0
Galcer 20:0(OH)/d18:1+Ag	878.5270	878.5288	1.6E+04	2.1
PC 40a:3+K	878.6036	878.6037	2.1E+03	0.1
2 Cholesterol+Ag	879.6143	879.6162	4.4E+04	2.2
PE 40p:6+Ag	882.4561	882.4573	5.1E+03	1.4
PE 36a:4-H+AgK	884.3756	884.3777	1.4E+03	2.4
Galcer 22:1/d18:2+Ag	886.5321	886.5336	1.2E+03	1.7
PE 36a:2-H+AgK	888.4069	888.4091	2.4E+04	2.4
PC 36a:4+Ag	888.4667	888.4669	5.4E+02	0.2
Galcer 22:1/d18:1 or 22:0/d18:2+Ag	888.5477	888.5498	3.7E+04	2.3
PE 36a:1-H+AgK	890.4226	890.4246	6.2E+04	2.3
Galcer 22:0/d18:1+Ag	890.5634	890.5652	3.4E+04	2.1
PE 38p:6-H+AgK	892.3807	892.3828	1.6E+04	2.3
PA40:6-H+AgK	893.3647	893.3670	5.3E+04	2.5
PE 38p:5-H+AgK	894.3964	894.3983	6.3E+03	2.1
PE 38p:4-H+AgK	896.4120	896.4141	4.4E+04	2.3
PE 40a:6+Ag	898.4511	898.4525	1.3E+04	1.6
Galcer 23:1/d18:1 or 23:0/d18:2+Ag	902.5634	902.5658	6.6E+03	2.7
Galcer 22:1(OH)/d18:1 or 22:0(OH)/d18:2+Ag	904.5426	904.5457	6.5E+04	3.4

Assignments	Theoretical m/z	m/z _{obs}	Counts	Error (ppm)
Galcer 23:0/d18:1+Ag	904.5790	904.5806	3.0E+03	1.7
Galcer 22:0(OH)/d18:1+Ag	906.5583	906.5602	2.7E+05	2.1
PE 38a:6-H+AgK	908.3756	908.3777	2.8E+04	2.3
PE 38a:5-H+AgK	910.3913	910.3926	7.4E+03	1.4
PE 38a:4-H+AgK	912.4069	912.4092	8.6E+04	2.5
Galcer 24:1/d18:2+Ag	914.5634	914.5653	7.2E+04	2.1
Galcer 24:1/d18:1 or 24:0/d18:2+Ag	916.5790	916.5810	3.4E+05	2.1
PE 40p:7-H+AgK	918.3964	918.3983	3.3E+03	2.1
Galcer 24:0/d18:1+Ag	918.5947	918.5966	1.0E+05	2.1
PE 40p:6-H+AgK	920.4120	920.4141	6.7E+04	2.3
Galcer 23:0(OH)/d18:1+Ag	920.5739	920.5763	8.0E+04	2.5
PE 40p:4-H+AgK	924.4433	924.4448	1.2E+04	1.6
PE 40e:4-H+AgK	926.4590	926.4625	8.8E+02	3.8
Galcer 24:1(OH)/d18:2+Ag	930.5583	930.5604	4.1E+04	2.2
Galcer 25:1/d18:1 or 25:0/18:2+Ag	930.5947	930.5964	1.9E+03	1.9
Galcer 24:1(OH)/d18:1 or 24:0(OH)/d18:2+Ag	932.5739	932.5758	4.5E+05	2.0
PE 40a:7-H+AgK	934.3913	934.3934	1.8E+04	2.2
Galcer 24:0(OH)/d18:1+Ag	934.5896	934.5910	7.0E+05	1.5
PE40a:6-H+AgK	936.4069	936.4090	1.5E+05	2.2
PE40a:4-H+AgK	940.4382	940.4400	1.5E+04	1.9

Supplementary table 2: Mass, assignment and intensity of peaks in negative ion mode, the different classes observed are PE, ST, PI and Galcer as deprotonated species, and SM-H-CH₂. PA are reported in red as they can have multiple origins

Assignments	Theoretical m/z	m/z _{obs}	Counts	Error (ppm)
PA 34:1-H	673.4814	673.4791	7.4E+04	-3.3
SM 16:0/d18:1-H-CH ₂	687.5441	687.5424	6.2E+03	-2.4
PA 36:2-H	699.4970	699.4946	6.1E+04	-3.4
PE 34p:1-H	700.5287	700.5258	8.5E+04	-4.1
PA 36:1-H	701.5127	701.5118	5.9E+04	-1.3
SM 18:1/d18:1 or 18:0/d18:2 -H-CH ₂	713.5592	713.5585	5.0E+03	-1.0
SM 18:0/d18:1-H-CH ₂	715.5749	715.5735	1.7E+05	-1.9
PE 34a:1-H	716.5236	716.5214	4.3E+04	-3.1
PE 34a:0-H	718.5392	718.5369	1.2E+05	-3.2
PA 38:5-H	721.4814	721.4801	1.3E+03	-1.7
PE 36p:4-H	722.5130	722.5102	2.3E+04	-3.9
PA 38:4-H	723.4970	723.4954	1.7E+04	-2.2
PE 36p:2-H	726.5443	726.5419	9.2E+04	-3.4
PE 36p:1-H	728.5600	728.5578	9.2E+04	-3.0
PE 36p:0-H	730.5756	730.5727	4.3E+03	-4.0
PE 36a:4-H	738.5079	738.5057	4.0E+03	-3.0
SM 20:1/d18:1 or 20:0/d18:2 -H-CH ₂	741.5910	741.5892	1.2E+03	-2.5
PE 36a:2-H	742.5392	742.5368	7.4E+04	-3.3
SM 20:0/d18:1-H-CH ₂	743.6067	743.6048	7.6E+03	-2.5
PE 36a:1-H	744.5549	744.5524	2.6E+05	-3.3
PE 38p:6-H	746.5130	746.5104	6.5E+04	-3.6
PE 36a:0-H	746.5705	746.5682	1.2E+04	-3.1
PA 40:6-H	747.4970	747.4941	6.9E+04	-3.9
PE 38p:4-H	750.5443	750.5418	8.9E+04	-3.3
PE 38p:2-H	754.5756	754.5730	4.3E+03	-3.5
PE 38a:6-H	762.5079	762.5053	6.9E+04	-3.5
PE 38a:5-H	764.5236	764.5213	2.1E+04	-3.0

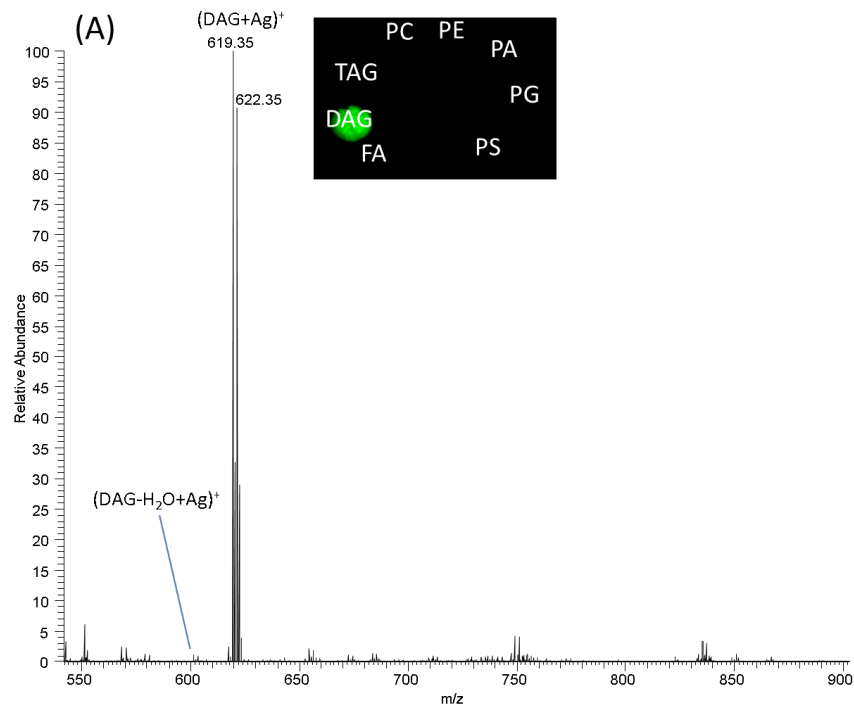
Assignments	Theoretical m/z	m/z _{obs}	Counts	Error (ppm)
PE 38a:4-H	766.5392	766.5369	1.9E+05	-3.1
SM 22:1/d18:1 or 22:0/d18:2 -H-CH ₂	769.6223	769.6203	2.2E+03	-2.6
PE 38a:2-H	770.5705	770.5678	2.5E+03	-3.5
SM 22:0/d18:1-H-CH ₂	771.6380	771.6360	4.7E+03	-2.7
PE 40p:7-H	772.5287	772.5260	9.1E+03	-3.5
PE 38a:1-H	772.5862	772.5836	3.7E+04	-3.4
PE 40p:6-H	774.5443	774.5418	1.3E+05	-3.2
PE 40p:4-H	778.5756	778.5733	1.2E+04	-3.0
PE 40a:7-H	788.5236	788.5205	4.2E+04	-3.8
PE 40a:6-H	790.5392	790.5365	2.2E+05	-3.4
PE 40a:4-H	794.5705	794.5681	2.3E+04	-3.0
SM 24:1/d18:1 or 24:0/d18:2 -H-CH ₂	797.6536	797.6516	1.5E+03	-2.6
SM 24:0/d18:1-H-CH ₂	799.6693	799.6671	1.5E+03	-2.7
ST 18:1/d18:1 or 18:0/d18:2 -H	804.5301	804.5275	4.9E+03	-3.3
ST 18:0/d18:1-H	806.5458	806.5433	1.3E+05	-3.1
PA 34:1-H+AgCl	815.3548	815.3538	8.3E+02	-1.2
ST 18:0(OH)/d18:1-H	822.5407	822.5424	1.9E+04	2.1
GalCer 24:1(OH)/d18:1 or 24:0(OH)/d18:2-H	824.6621	824.6589	7.7E+02	-3.8
GalCer 24:0(OH)/d18:1-H	826.6778	826.6748	3.1E+03	-3.6
ST 20:0/d18:1-H	834.5771	834.5746	3.1E+03	-3.0
ST 20:0(OH)/d18:1-H	850.5720	850.5692	1.0E+03	-3.3
PI 36:4-H	857.5186	857.5151	7.0E+04	-4.1
PE 34a:0-H+AgCl	860.4126	860.4137	2.7E+03	1.2
ST 22:1/d18:1 or 22:0/18:2-H	860.5927	860.5901	4.6E+03	-3.0
ST C22:0/d18:1-H	862.6084	862.6058	2.2E+04	-3.0
PE36p:2-H+AgCl	868.4177	868.4164	8.2E+02	-1.5
ST 22:1(OH)/d18:1 or 22:0(OH)/18:2 -H	876.5876	876.5867	6.2E+03	-1.0

Assignments	Theoretical m/z	m/z _{obs}	Counts	Error (ppm)
ST 22:0(OH)/d18:1-H	878.6033	878.6006	6.6E+04	-3.1
PI 38:6-H	881.5186	881.5159	1.4E+03	-3.1
PI 38:5-H	883.5342	883.5314	3.8E+04	-3.1
PE 36a:2-H+AgCl	884.4126	884.4122	4.4E+02	-0.4
PI 38:4-H	885.5499	885.5473	4.0E+05	-2.9
PE36a:1-H+AgCl	886.4283	886.4285	2.4E+04	0.3
ST 24:1/d18:2-H	886.6084	886.6054	4.0E+04	-3.3
ST 24:1/d18:1 or 24:0/18:2 -H	888.6240	888.6214	2.8E+05	-3.0
PA 40:6-H+AgCl	889.3704	889.3692	6.0E+02	-1.3
ST 24:0/d18:1-H	890.6397	890.6371	1.4E+05	-2.9
PE 38p:4-H+AgCl	892.4177	892.4131	5.1E+02	-5.2
ST 24:1(OH)/d18:2-H	902.6033	902.6023	1.3E+04	-1.1
PE 38a:6-H+AgCl	904.3813	904.3791	5.8E+02	-2.5
ST 24:1(OH)/d18:1 or 24:0(OH)/18:2 -H	904.6189	904.6164	1.6E+05	-2.8
ST 24:0(OH)/d18:1-H	906.6346	906.6322	1.8E+05	-2.7
PE 38a:4-H+AgCl	908.4126	908.4122	1.2E+04	-0.5
PI 40:6-H	909.5498	909.5474	1.7E+03	-2.6
PE 40p:6-H+AgCl	916.4177	916.4208	7.1E+03	3.4
PE 40a:6-H+AgCl	932.4126	932.4123	1.7E+04	-0.4

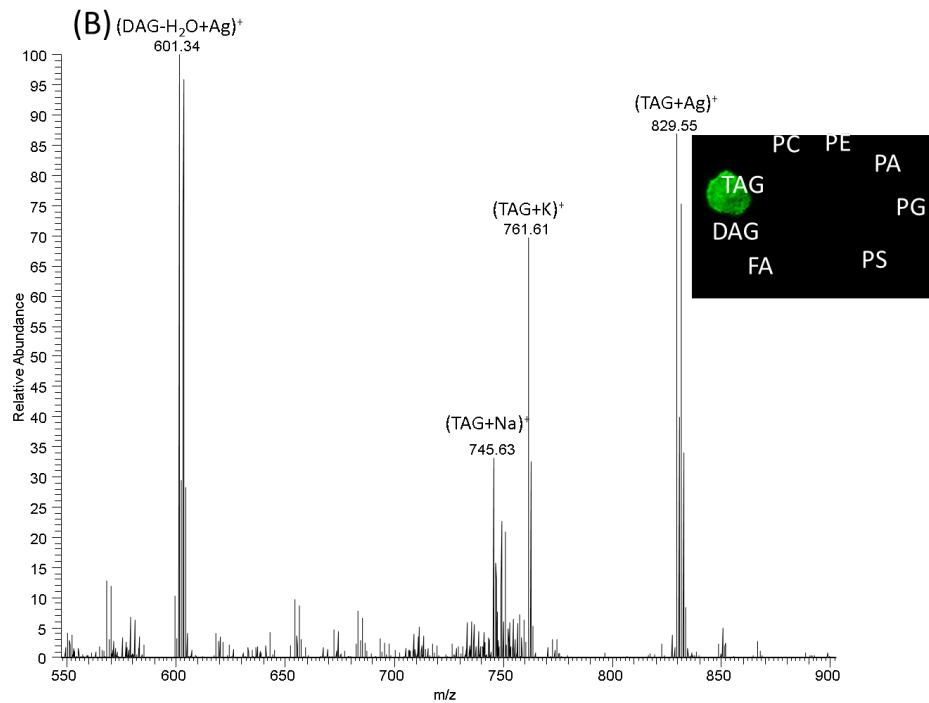
Supplementary table 3: Intensity and coefficient of variation from lipids peak in 4 successive tissue sections sorted by lipids class and cationization

<u>Lipid species</u>	<u>Lipid assignment</u>	<u>Exact Mass</u>	<u>CV 25%</u>	<u>CV 50%</u>	<u>CV 75%</u>	<u>CV 90%</u>
PE(NaK)	<u>PE36a:1-H+NaK</u>	<u>806.5073</u>	<u>0.2381</u>	<u>0.1567</u>	<u>0.1361</u>	<u>0.1276</u>
	<u>PE38a:4-H+NaK</u>	<u>828.4916</u>	<u>(all zeros)</u>	<u>0.1823</u>	<u>0.1236</u>	<u>0.1186</u>
	<u>PE40a:6-H+NaK</u>	<u>852.4916</u>	<u>(all zeros)</u>	<u>(all zeros)</u>	<u>0.1209</u>	<u>0.1394</u>
	<u>Across PE(NaK) average CV</u>			<u>0.1695</u>	<u>0.1269</u>	<u>0.1285</u>
PE(2K)	<u>PE36a:1-H+2K</u>	<u>822.4812</u>	<u>0.2357</u>	<u>0.1936</u>	<u>0.1751</u>	<u>0.1678</u>
	<u>PE38a:4-H+2K</u>	<u>844.4656</u>	<u>0.2027</u>	<u>0.1531</u>	<u>0.1386</u>	<u>0.1379</u>
	<u>PE40a:6-H+2K</u>	<u>868.4656</u>	<u>0.1647</u>	<u>0.1513</u>	<u>0.1437</u>	<u>0.1598</u>
	<u>Across PE(2K) average CV</u>			<u>0.201</u>	<u>0.166</u>	<u>0.1525</u>
PE(AgK)	<u>PE36a:1-H+AgK(Ag109)</u>	<u>892.4231</u>	<u>0.1667</u> <u>excluding</u> <u>one zero</u>	<u>0.1462</u>	<u>0.1241</u>	<u>0.1097</u>
	<u>PE38a:4-H+AgK</u>	<u>912.4069</u>	<u>0.1376</u>	<u>0.0907</u>	<u>0.0772</u>	<u>0.0791</u>
	<u>PE40a:6-H+AgK</u>	<u>936.4069</u>	<u>0.1036</u>	<u>0.0958</u>	<u>0.0856</u>	<u>0.0929</u>
	<u>Across PE(AgK) average CV</u>			<u>0.136</u>	<u>0.1109</u>	<u>0.0956</u>
GalCer(Na)	<u>GalCer C22:0(OH)/d18:1+Na</u>	<u>822.643</u>	<u>(all zeros)</u>	<u>(all zeros)</u>	<u>0.1758</u>	<u>0.1546</u>
	<u>GalCer C24:1(OH)/d18:1+Na</u>	<u>848.6586</u>	<u>(all zeros)</u>	<u>0.1611</u>	<u>0.1446</u>	<u>0.1391</u>
	<u>GalCer C24:0(OH)/d18:1+Na</u>	<u>850.6743</u>	<u>(all zeros)</u>	<u>0.1474</u>	<u>0.1412</u>	<u>0.1368</u>
	<u>Across GalCer(Na) average CV</u>			<u>0.1542</u>	<u>0.1539</u>	<u>0.1435</u>
GalCer(K)	<u>GalCer C22:0(OH)/d18:1+K</u>	<u>838.6169</u>	<u>(all zeros)</u>	<u>(all zeros)</u>	<u>0.088</u>	<u>0.144</u>
	<u>GalCer C24:1(OH)/d18:1+K</u>	<u>864.6325</u>	<u>(all zeros)</u>	<u>0.1318</u>	<u>0.1274</u>	<u>0.1334</u>
	<u>GalCer C24:0(OH)/d18:1+K</u>	<u>866.6482</u>	<u>(all zeros)</u>	<u>0.1242</u>	<u>0.119</u>	<u>0.1373</u>
	<u>Across GalCer(K) average CV</u>			<u>0.128</u>	<u>0.1115</u>	<u>0.1382</u>
GalCer(Ag)	<u>GalCer C22:0(OH)/d18:1+Ag (Ag109)</u>	<u>908.5601</u>	<u>(all zeros)</u>	<u>0.0502</u>	<u>0.034</u>	<u>0.0319</u>
	<u>GalCer C24:1(OH)/d18:1+Ag</u>	<u>932.5739</u>	<u>0.139</u>	<u>0.0389</u>	<u>0.0283</u>	<u>0.0268</u>
	<u>GalCer C24:0(OH)/d18:1+Ag (Ag109)</u>	<u>936.5917</u>	<u>0.1264</u>	<u>0.0468</u>	<u>0.0376</u>	<u>0.038</u>
	<u>Across GalCer(Ag) average CV</u>			<u>0.1328</u>	<u>0.0453</u>	<u>0.0333</u>
Cer(Ag)	<u>Cer C18:1/d18:1+Ag</u>	<u>670.4323</u>	<u>(all zeros)</u>	<u>(all zeros)</u>	<u>0.1295</u>	<u>0.1238</u>
	<u>Cer C18:0/d18:1+Ag</u>	<u>672.4479</u>	<u>0.1622</u>	<u>0.1154</u>	<u>0.1056</u>	<u>0.1067</u>
	<u>Cer C20:0/d18:1+Ag</u>	<u>700.4792</u>	<u>(all zeros)</u>	<u>(all zeros)</u>	<u>(all zeros)</u>	<u>0.1244</u>
	<u>Across Cer(Ag) average CV</u>				<u>0.1176</u>	<u>0.1183</u>
DAG(Ag)	<u>DAG 36a:1+Ag</u>	<u>729.4582</u>	<u>(all zeros)</u>	<u>(all zeros)</u>	<u>0.0506</u>	<u>0.0323</u>
	<u>DAG 38a:4+Ag</u>	<u>751.4425</u>	<u>(all zeros)</u>	<u>(half zeros)</u>	<u>0.1267</u>	<u>0.0316</u>
	<u>DAG 40a:6+Ag</u>	<u>775.4425</u>	<u>(all zeros)</u>	<u>(all zeros)</u>	<u>(all zeros)</u>	<u>0.0396</u>
	<u>Across DAG(Ag) average CV</u>				<u>0.0886</u>	<u>0.0345</u>
Cer-H2O(Ag)	<u>Cer C18:1/d18:1-H2O+Ag</u>	<u>652.4223</u>	<u>0.1191</u> <u>excluding</u> <u>one zero</u>	<u>0.095</u>	<u>0.0812</u>	<u>0.0806</u>
	<u>Cer C18:0/d18:1-H2O+Ag</u>	<u>656.4384</u>	<u>0.0943</u>	<u>0.0641</u>	<u>0.0507</u>	<u>0.0441</u>
	<u>Cer C24:1/d18:1-H2O+Ag</u>	<u>736.5162</u>	<u>(all zeros)</u>	<u>0.0972</u>	<u>0.0711</u>	<u>0.0557</u>
	<u>Across Cer-H2O(Ag) average CV</u>			<u>0.1067</u>	<u>0.0854</u>	<u>0.0677</u>

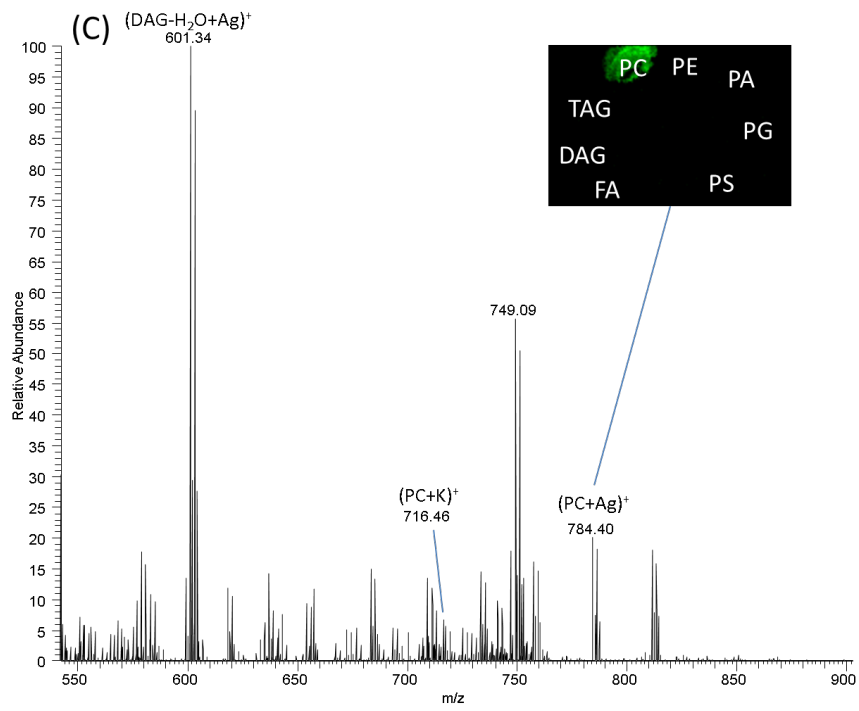
Supplementary figure 1: Positive ion mode spectra of lipid standards on rat brain tissue implanted with AgNP and MALDI images extracted from one of the major cationization



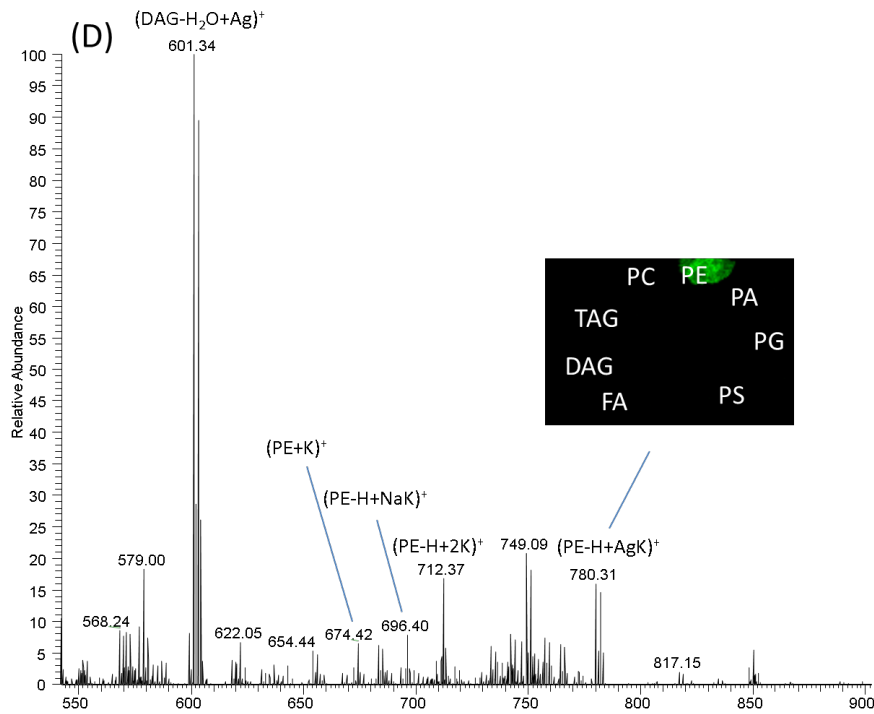
Supplementary figure 1A: Positive ion mode spectra of DAG standard on rat brain tissue implanted with AgNP and MALDI images extracted for the m/z 619.35 corresponding to DAG(28:0)+Ag.



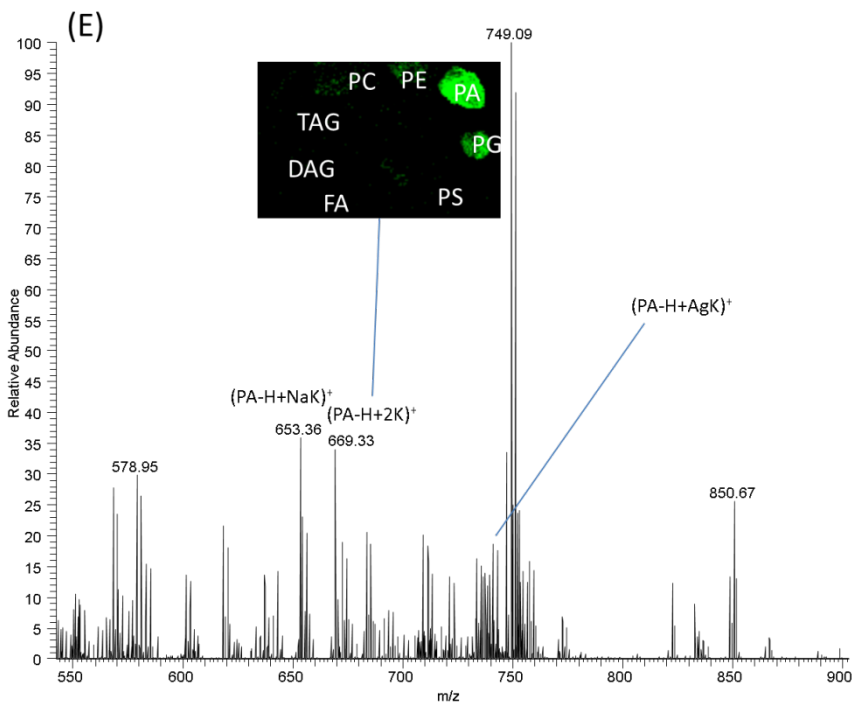
Supplementary figure 1B: Positive ion mode spectra of TAG standard on rat brain tissue implanted with AgNP and MALDI images extracted for the m/z 829.55 corresponding to TAG(42:0)+Ag.



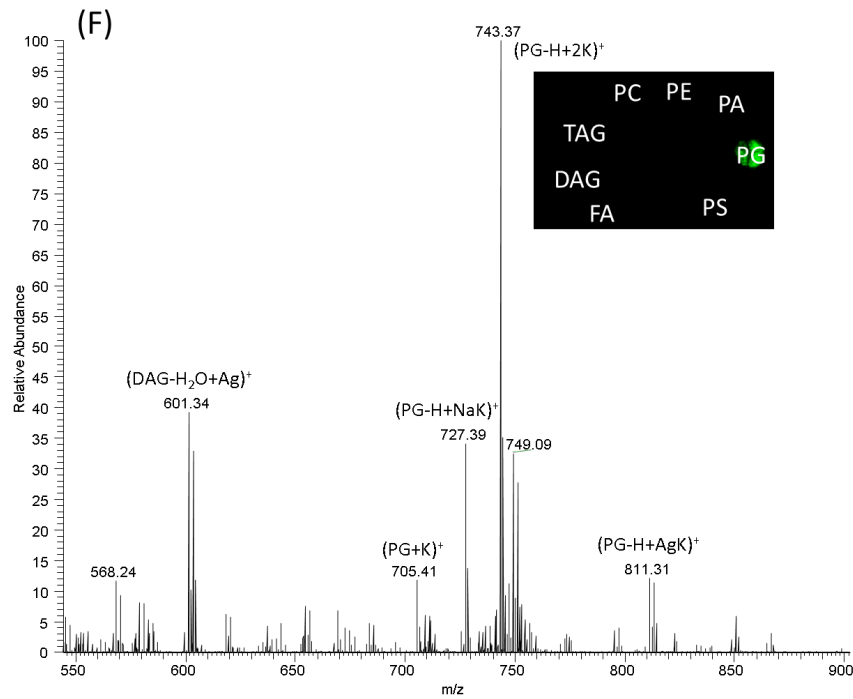
Supplementary figure 1C: Positive ion mode spectra of PC standard on rat brain tissue implanted with AgNP and MALDI images extracted for the m/z 784.40 corresponding to PC(28:0)+Ag.



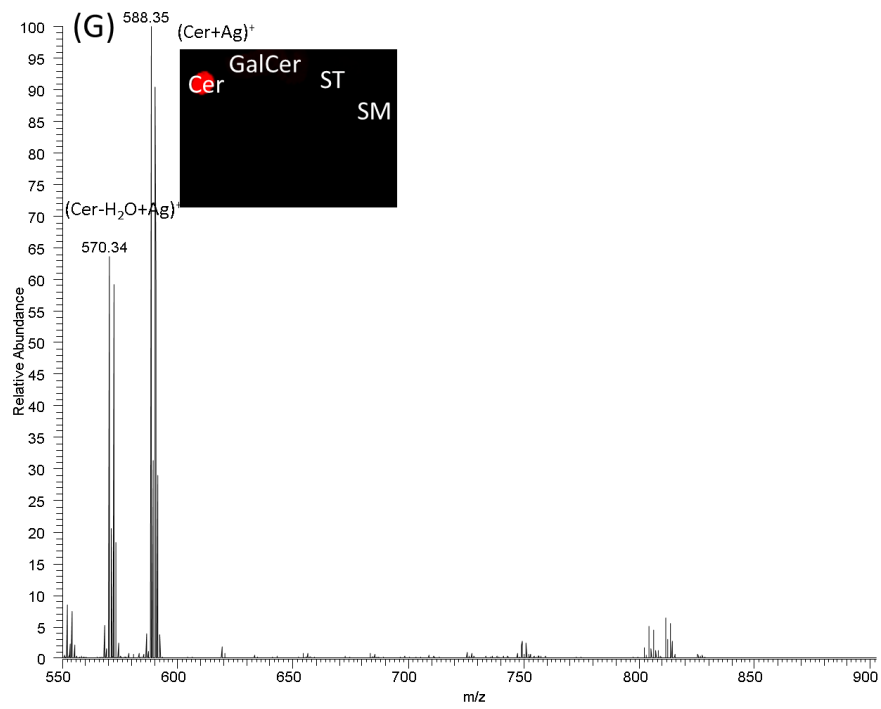
Supplementary figure 1D: Positive ion mode spectra of PE standard on rat brain tissue implanted with AgNP and MALDI images extracted for the m/z 780.31 corresponding to PE(28:0)-H+AgK.



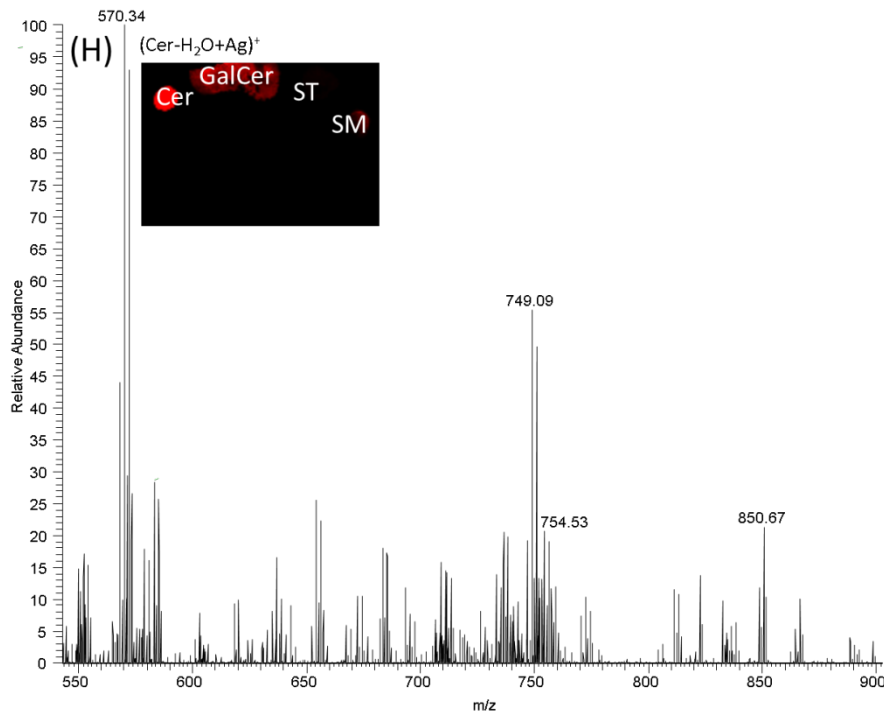
Supplementary figure 1E: Positive ion mode spectra of PA standard on rat brain tissue implanted with AgNP and MALDI images extracted for the m/z 669.33 corresponding to PA (28:0)-H+2K. This peak is present in PA, PG, PE and at low intensity in PC.



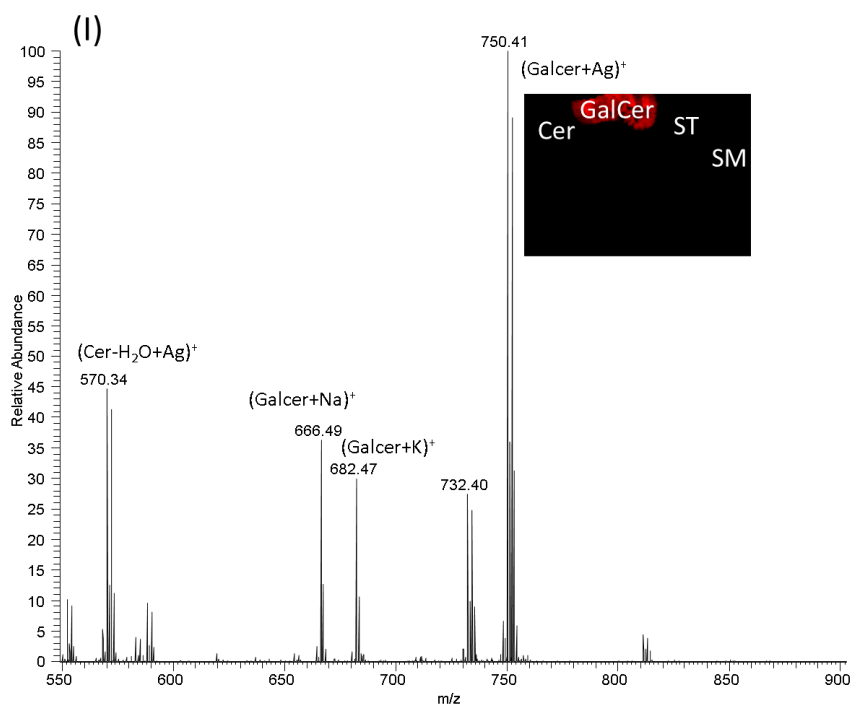
Supplementary figure 1F: Positive ion mode spectra of PG standard on rat brain tissue implanted with AgNP and MALDI images extracted for the m/z 743.37 corresponding to PG (28:0)-H+2K.



Supplementary figure 1G: Positive ion mode spectra of Cer standard on rat brain tissue implanted with AgNP and MALDI images extracted for the m/z 588.35 corresponding to Cer(12:0/d18:1)+Ag.

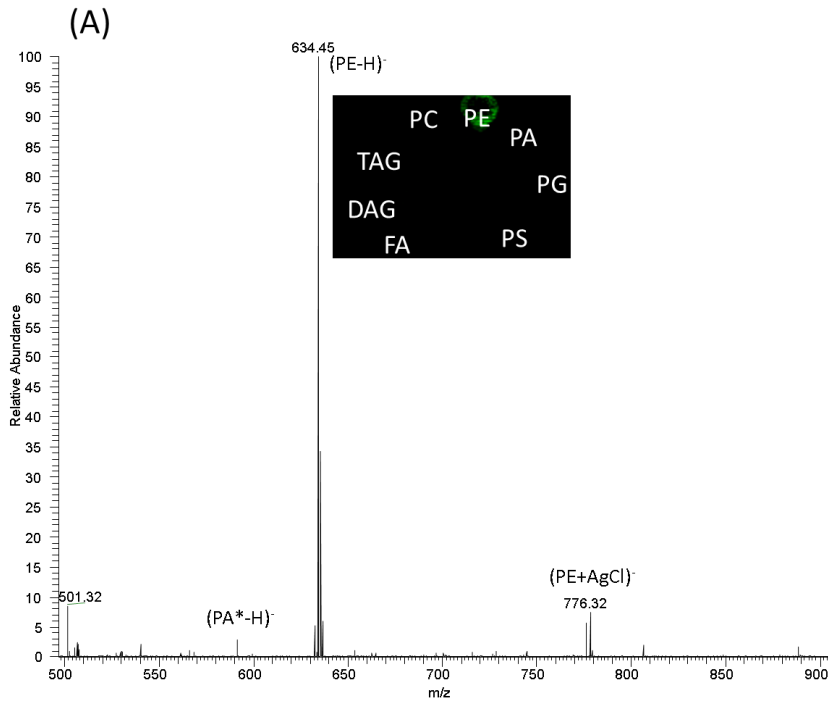


Supplementary figure 1H: Positive ion mode spectra of SM standard on rat brain tissue implanted with AgNP and MALDI images extracted for the m/z 570.34 corresponding to Cer(12:0/d18:1)-H₂O+Ag. This peak is present in Cer, Galcer and SM.

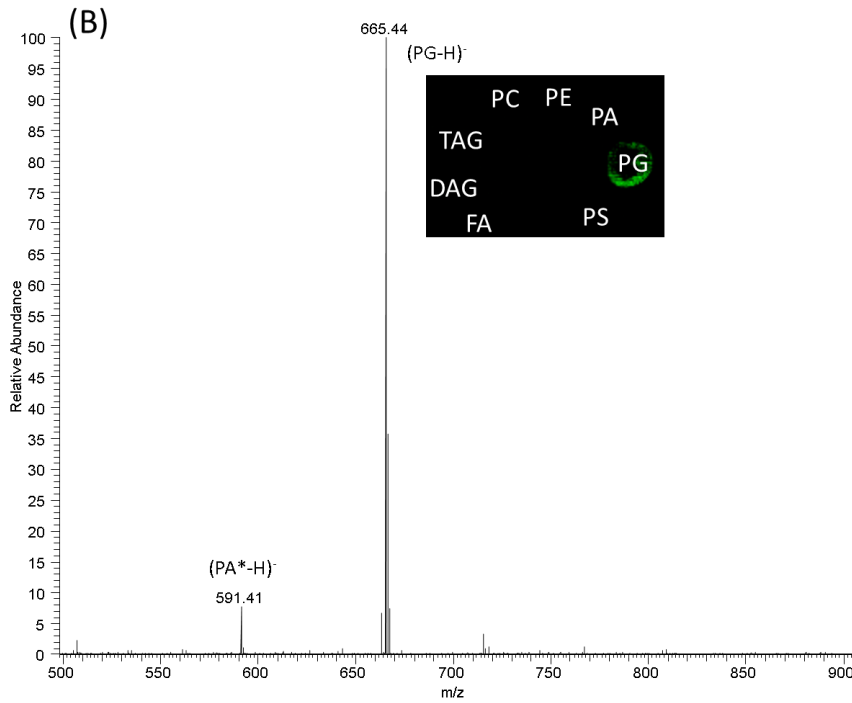


Supplementary figure 1I: Positive ion mode spectra of Galcer standard on rat brain tissue implanted with AgNP and MALDI images extracted for the m/z 750.41 corresponding to Galcer(12:0/d18:1)+Ag.

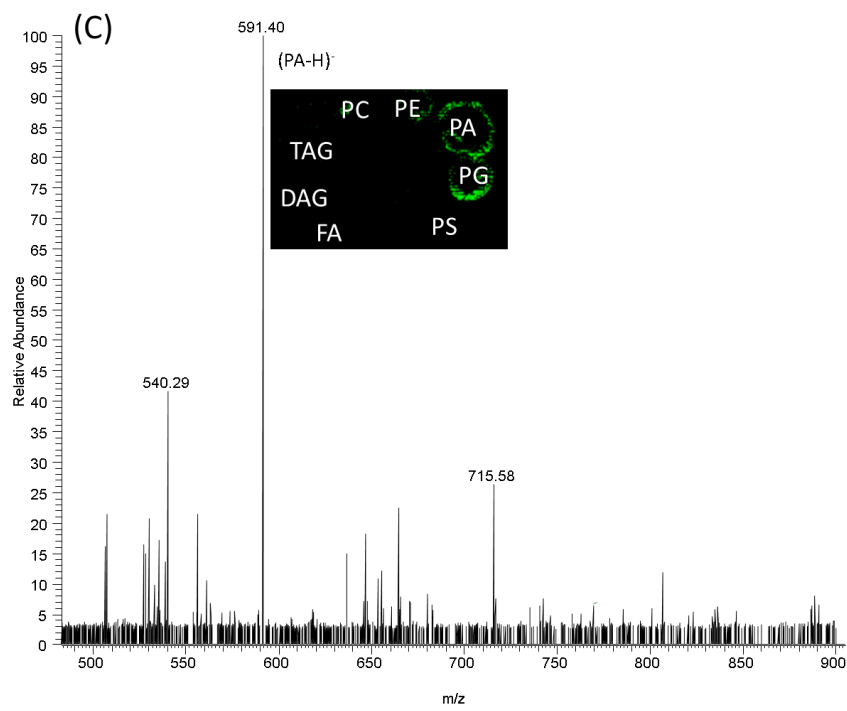
Supplementary figure 2: Negative ion mode spectra of standard on rat brain tissue implanted with AgNP and MALDI images extracted from deprotonated ion



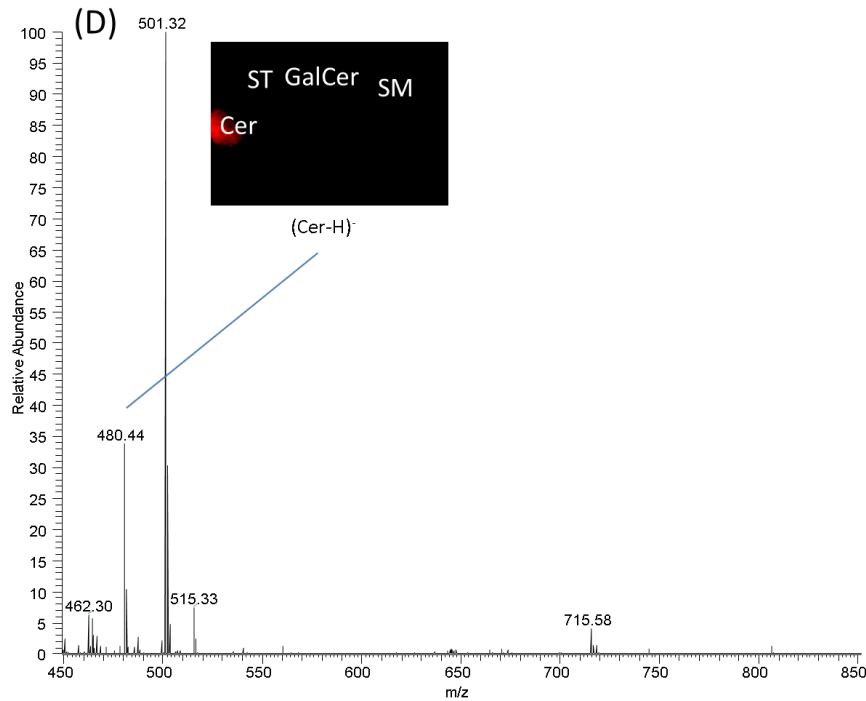
Supplementary figure 2A: Negative ion mode spectra of PE standard on rat brain tissue implanted with AgNP and MALDI images extracted for the m/z 634.45 corresponding to PE(28:0)-H. PA* can also correspond to fragment of other phospholipids.



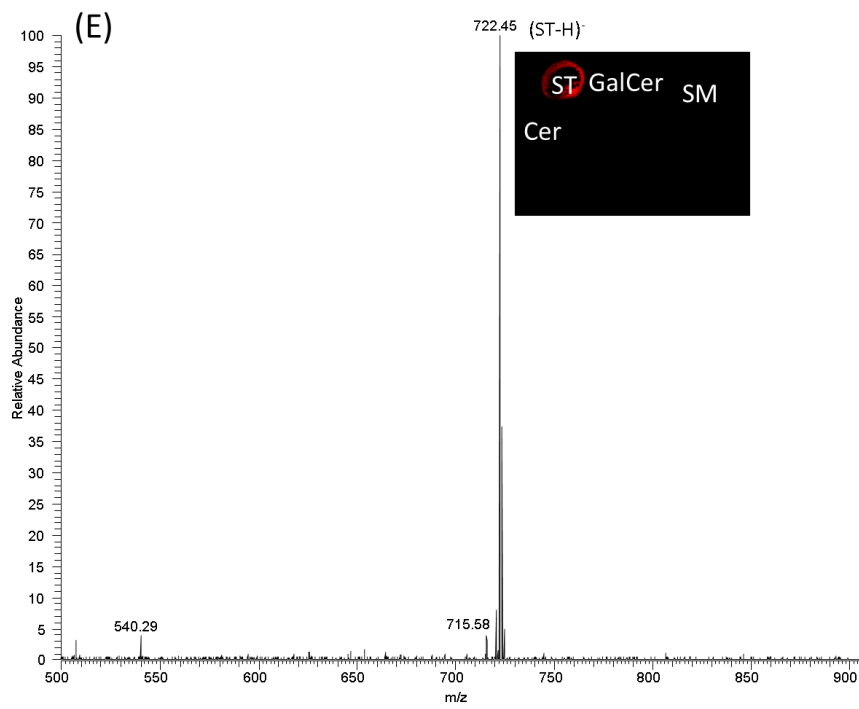
Supplementary figure 2B: Negative ion mode spectra of PG standard on rat brain tissue implanted with AgNP and MALDI images extracted for the m/z 665.44 corresponding to PG(28:0)-H. PA* can also correspond to fragment of other phospholipids.



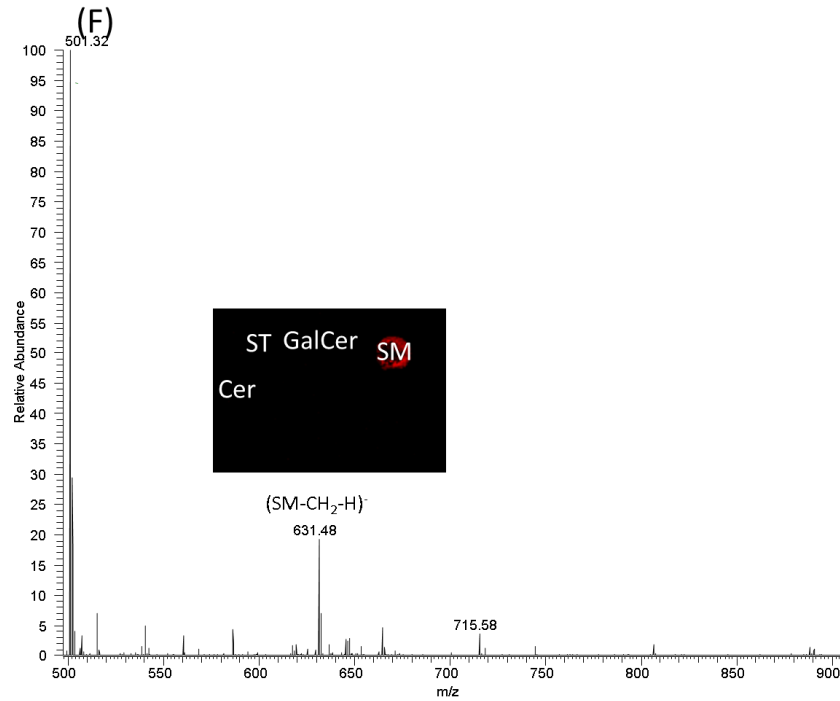
Supplementary figure 2C: Negative ion mode spectra of PA standard on rat brain tissue implanted with AgNP and MALDI images extracted for the m/z 665.44 corresponding to PA(28:0)-H. This peak is present in PG, PA, and at low intensity in PE and PC.



Supplementary figure 2D: Negative ion mode spectra of Cer standard on rat brain tissue implanted with AgNP and MALDI images extracted for the m/z 480.44 corresponding to Cer(12:0/d18:1)-H.

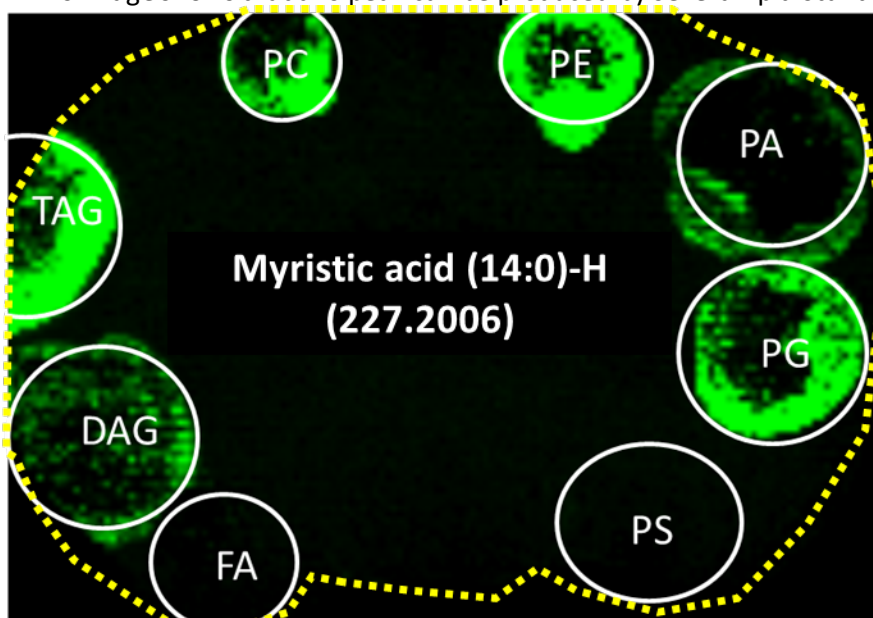


Supplementary figure 2E: Negative ion mode spectra of ST standard on rat brain tissue implanted with AgNP and MALDI images extracted for the m/z 480.44 corresponding to ST(12:0/d18:1)-H.



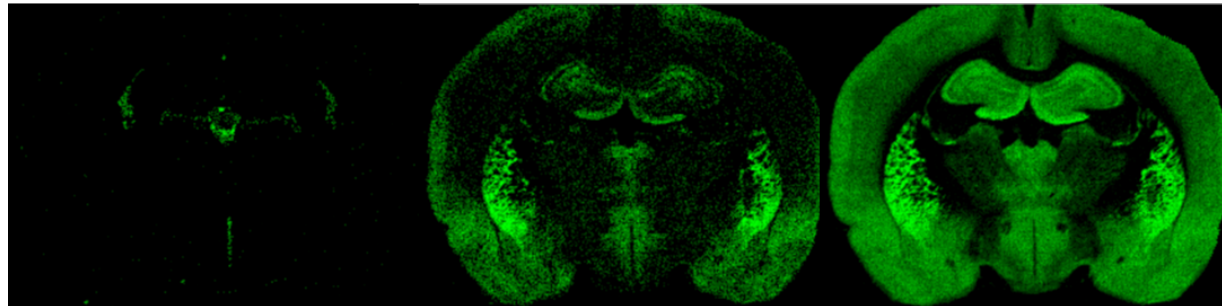
Supplementary figure 2F: Negative ion mode spectra of SM standard on rat brain tissue implanted with AgNP and MALDI images extracted for the m/z 480.44 corresponding to SM(12:0/d18:1)- CH_2 -H.

Supplementary figure 3: MALDI images in negative ion mode from deposited lipids on a rat brain section, the image has been extracted for the m/z 227.2006 corresponding to Myristic Acid(14:0)-H. This image shows that this peak can be produced by several lipid standards



Supplementary figure 4: MALDI images extracted for all lipids species identified in positive and negative ion mode. In positive ion mode all images shown are produced from silver cationization while in negative ion mode they are produced from M-H peak except for SM in which M-H-CH2 was used.

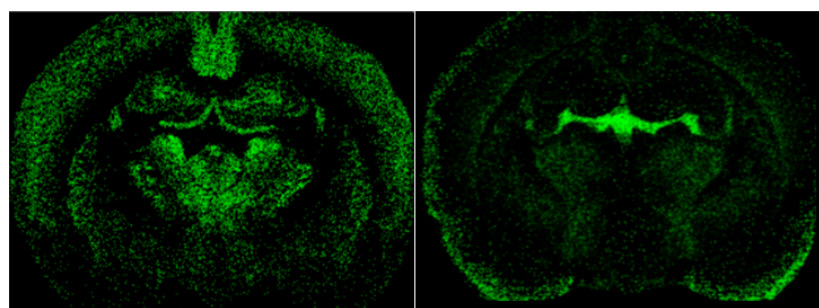
Ceramides (Cer)
Positive ion mode
 $(M+Ag)^+$



Cer C16:0/d18:1
644.42

Cer C18:1/d18:1
or C18:0/d18:2
670.43

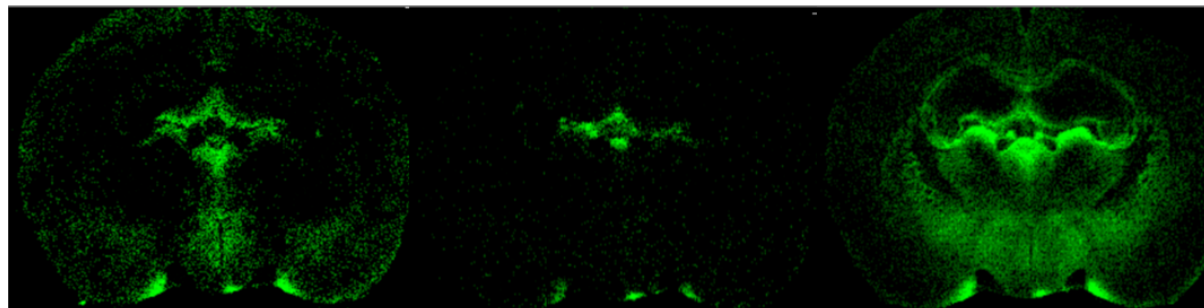
Cer C18:0/d18:1
672.45



Cer C20:0/d18:1
700.48

Cer C24:0/d18:1
756.54

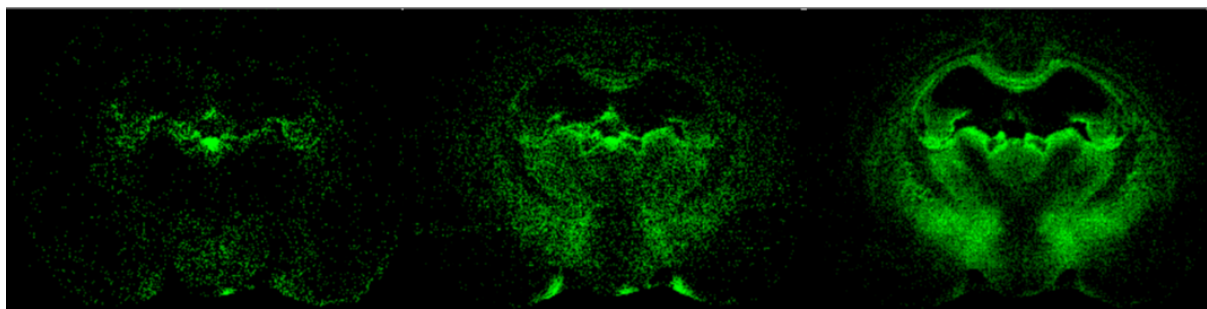
Diacylglycerols (DAG)
Positive ion mode
 $(M+Ag)^+$



DAG 32a:0
675.41

DAG 34a:0
699.41

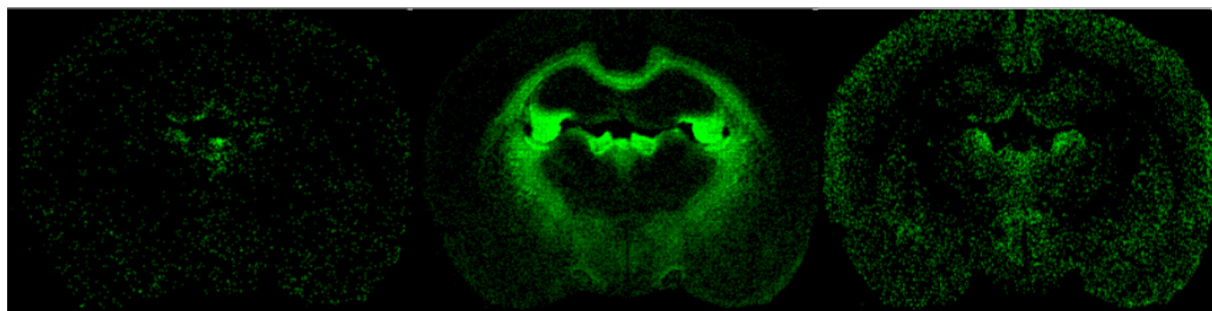
DAG 34a:1
701.43



DAG 36a:4
723.41

DAG 36a:2
727.44

DAG 36a:1
729.46

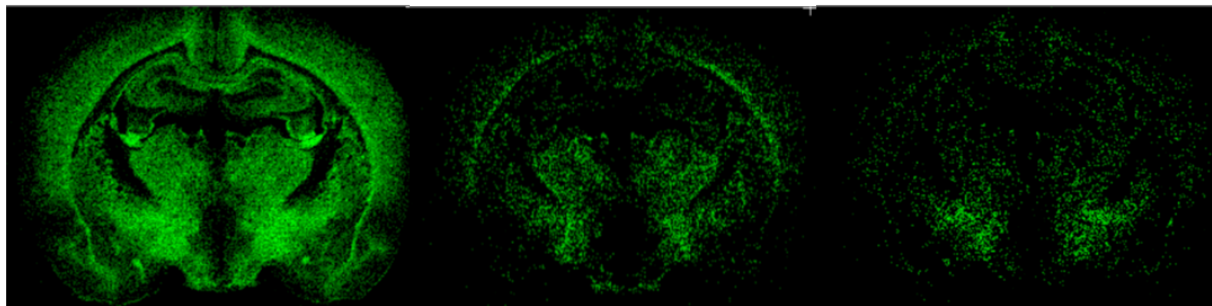


DAG 38a:6
747.41

DAG 38a:4
751.44

DAG 40a:6
775.44

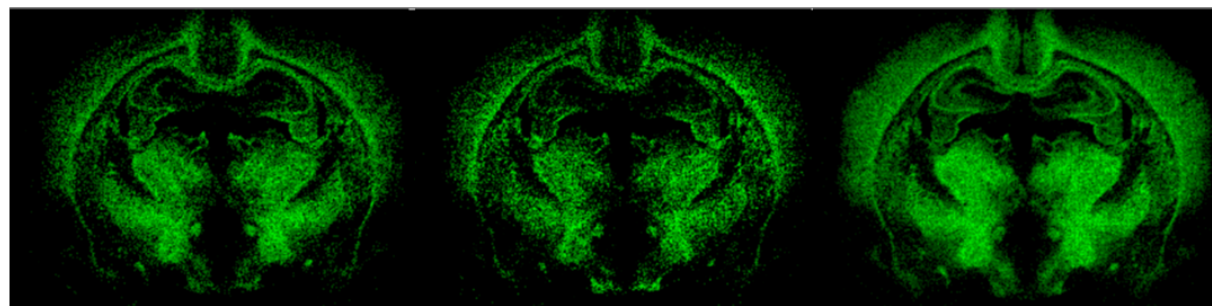
Galactoceramides (GalCer)
Positive ion mode
 $(M+Ag)^+$



Galcer C18:0/d18:1
834.50

Galcer C20:0/d18:1
862.53

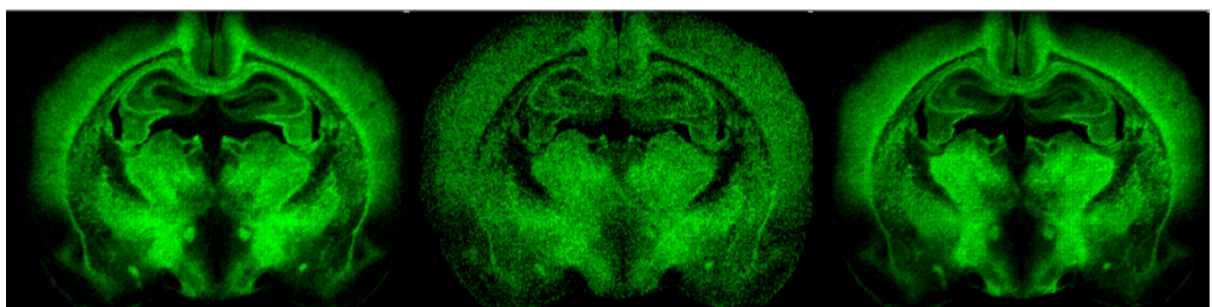
Galcer C20:0/d18:1(OH)
878.53



Galcer C22:1/d18:1
or C22:0/d18:2
888.55

Galcer C22:0/d18:1
890.56

Galcer C22:1(OH)/d18:1
or C22:0(OH)/d18:2
904.54

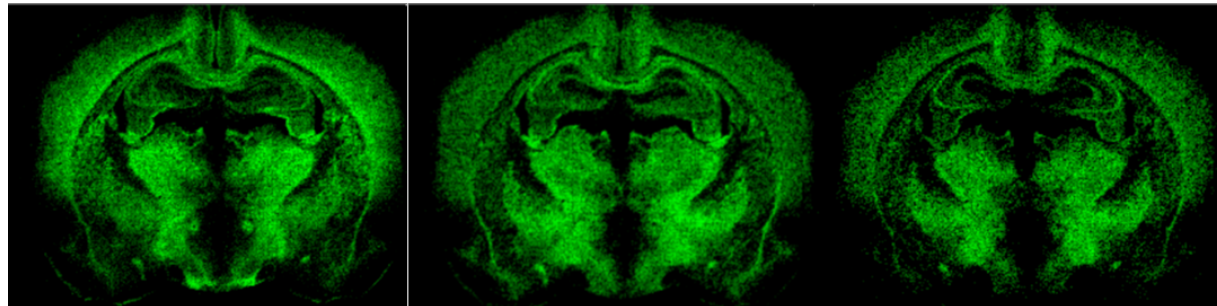


Galcer C22:0(OH)/d18:1
906.56

Galcer C24:1/d18:2
914.56

Galcer C24:1/d18:1
or C24:0/d18:2
916.58

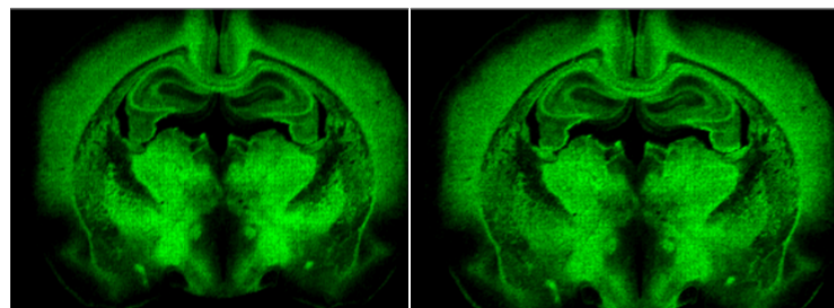
Galactoceramides (GalCer)
Positive ion mode
(M+Ag)⁺



GalCer C24:0/d18:1
918.59

Galcer C23:0(OH)/d18:1
920.57

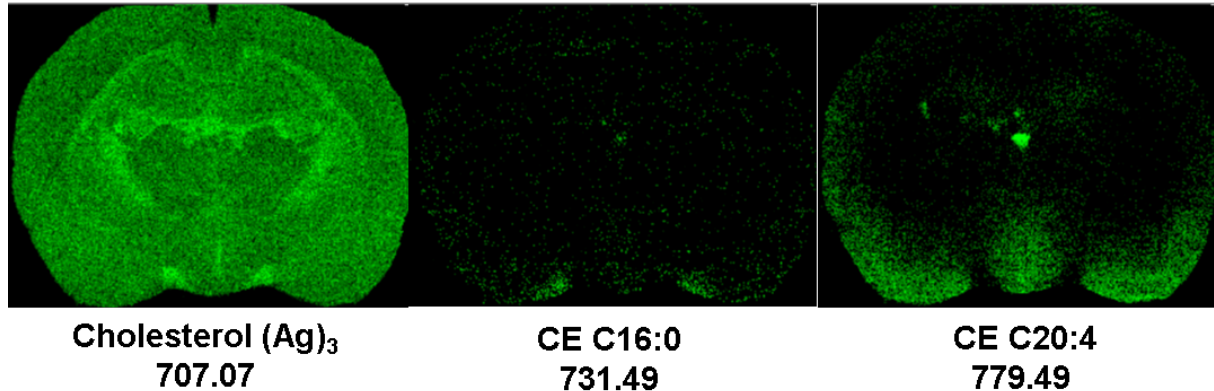
Galcer C24:1(OH)/d18:2
930.56



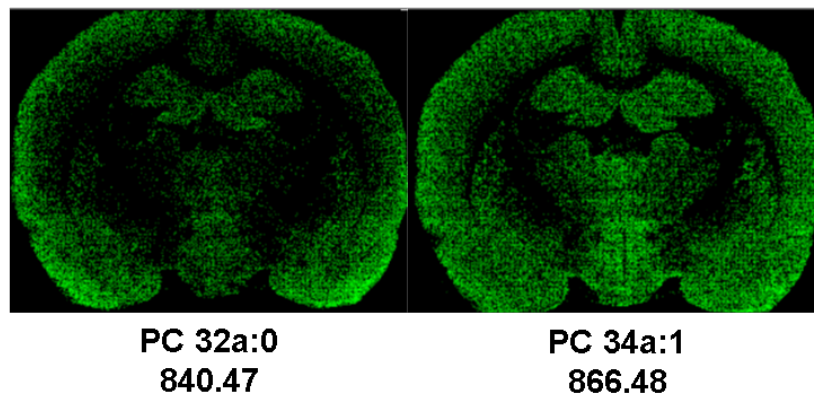
Galcer C24:1(OH)/d18:1
or C24:0(OH)/d18:2
932.57

Galcer C24:0(OH)/d18:1
934.59

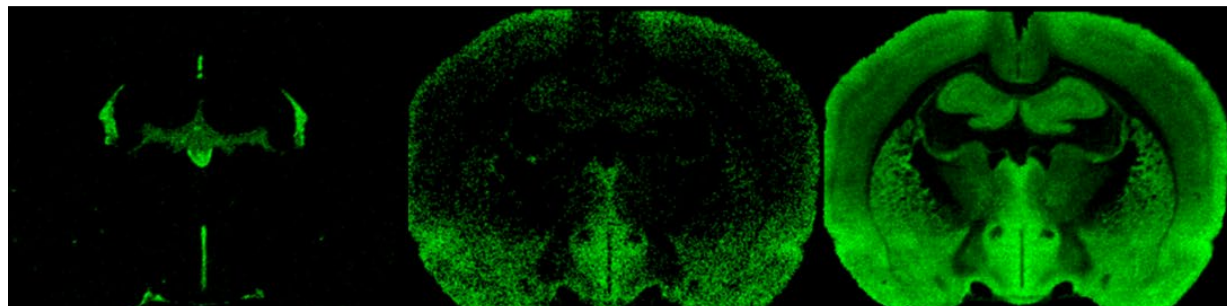
Cholesterol and cholesterol ester (CE)
Positive ion mode
 $M+(Ag)_3^+$ or $(M+Ag)^+$



Phosphatidylcholine (PC)
Positive ion mode
 $(M+Ag)^+$



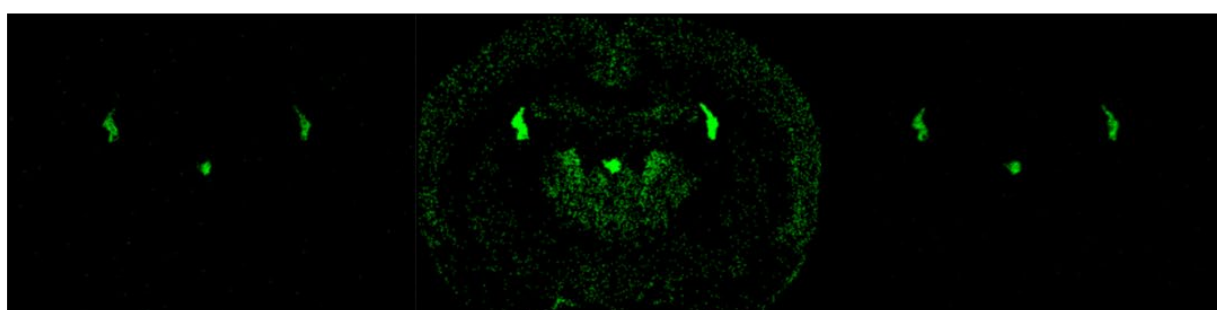
Sphingomyelin (SM)
Negative ion mode
(M-CH₂-H)⁻



SM C16:0/d18:1
687.54

SM C18:1/d18:1
or C18:0/d18:2
713.56

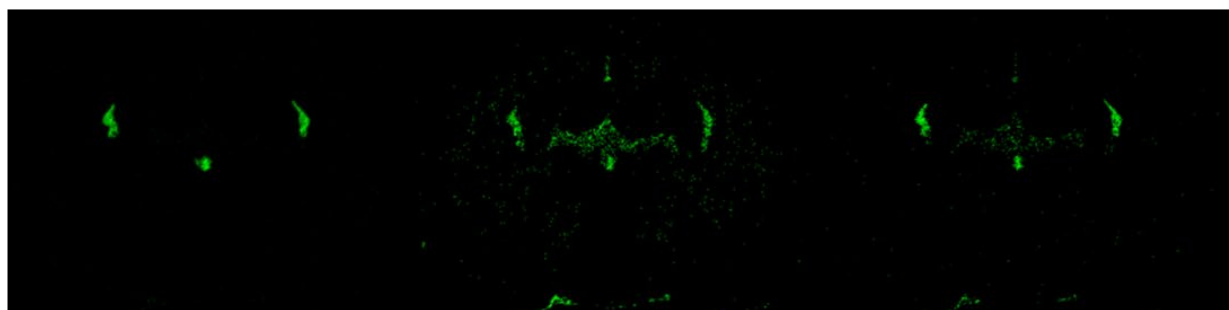
SM C18:0/d18:1
715.58



SM C20:1/d18:1
741.59

SM C20:0/d18:1
743.60

SM C22:1/d18:1
or C22:0/d18:2
769.62

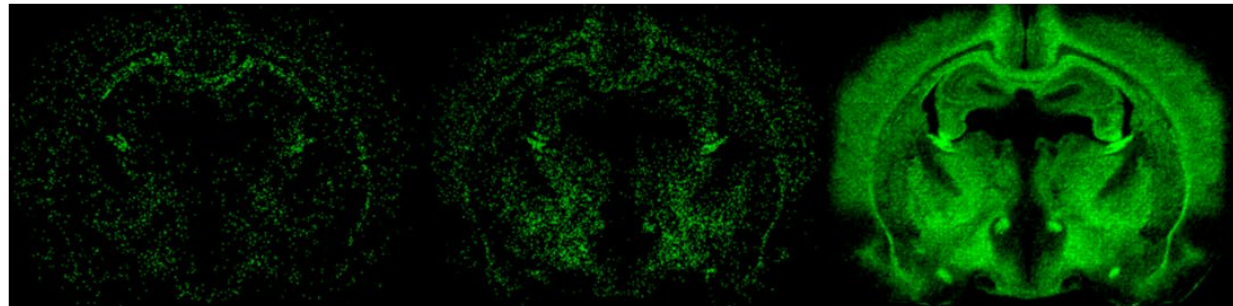


SM C22:0/d18:1
771.64

SM C24:1/d18:1
or C24:0/d18:2
797.65

SM C24:0/d18:1
799.67

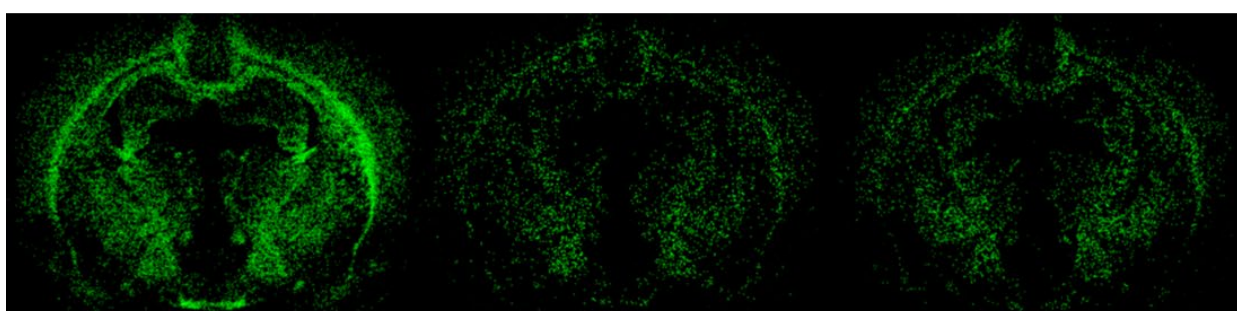
Sulfatide (ST)
Negative ion mode
(M-H)⁻



ST C16:0/d18:1
778.51

ST C18:1/d18:1
or C18:0/d18:2
804.53

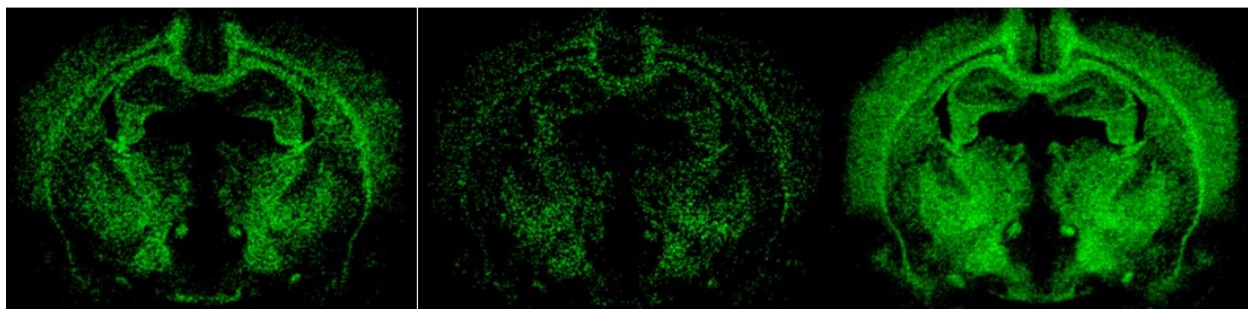
ST C18:0/d18:1
806.54



ST C18:0(OH)/d18:1
822.54

ST C20:0/d18:1
834.57

ST C22:1/d18:1
or C22:0/d18:2
860.59

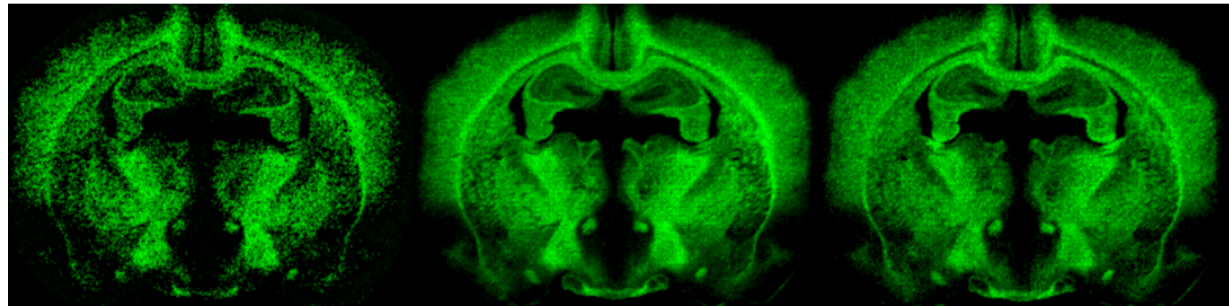


ST C22:0/d18:1
862.61

ST C22:1(OH)/d18:1
Or C 22:0(OH)/d18:2
876.58

ST C22:0(OH)/d18:1
878.60

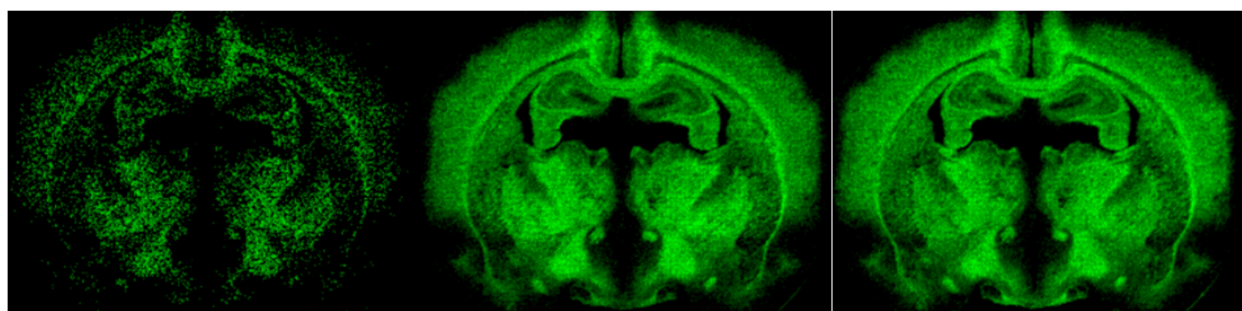
Sulfatide (ST)
Negative ion mode
(M-H)⁻



ST C24:1/d18:2
886.60

ST C24:1/d18:1
or C24:0/d18:2
888.62

ST C24:0/d18:1
890.63

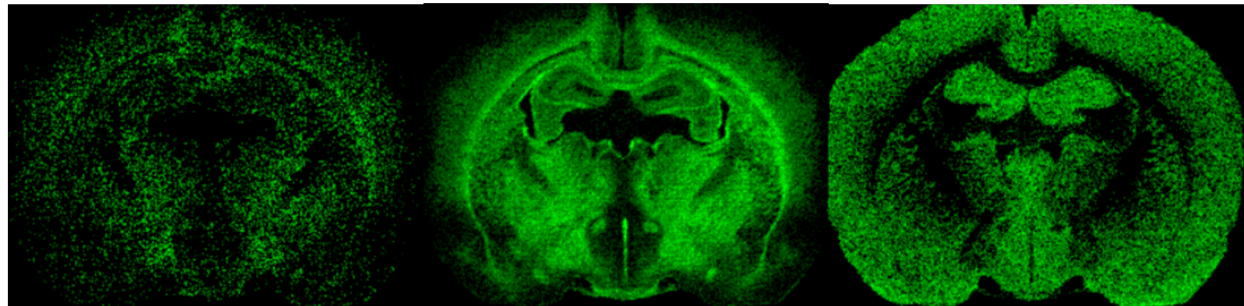


ST C24:1(OH)/d18:2
902.60

ST C24:1(OH)/d18:1
Or C24:0(OH)/d18:2
904.62

ST C24:0(OH)/d18:1
906.63

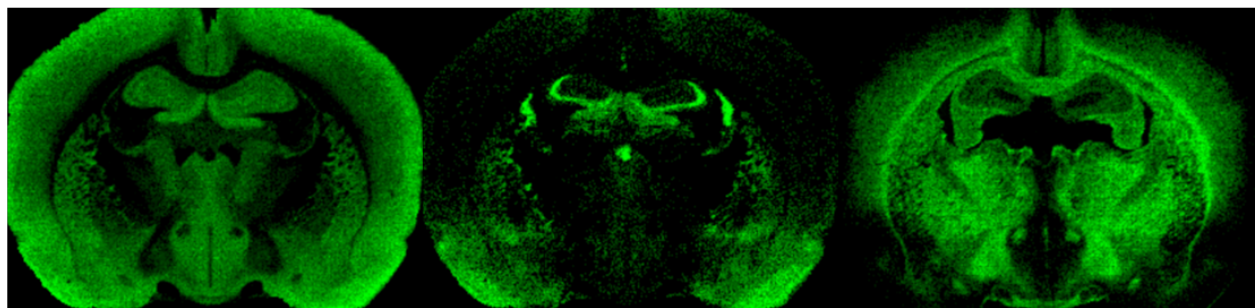
Phosphatidylethanol (PE)
Negative ion mode
(M-H)⁻



PE 34p:1
700.52

PE 34p:0
702.54

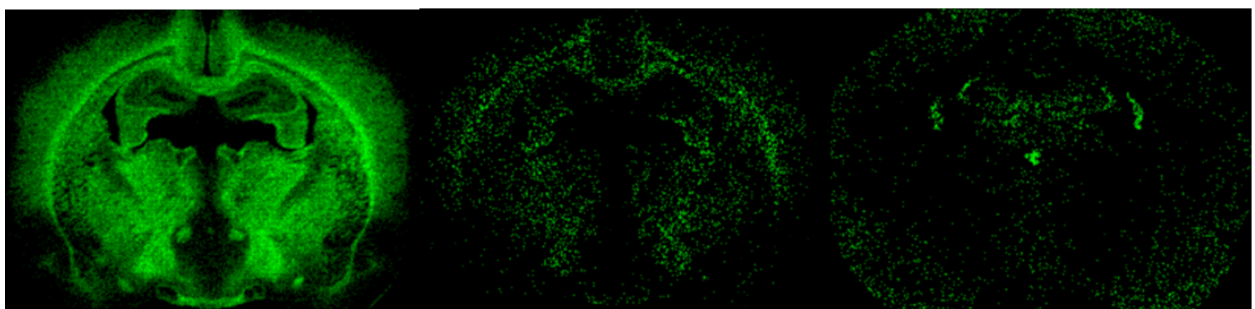
PE 34a:1
716.52



PE 34a:0
718.54

PE 36p:4
722.51

PE 36p:2
726.54

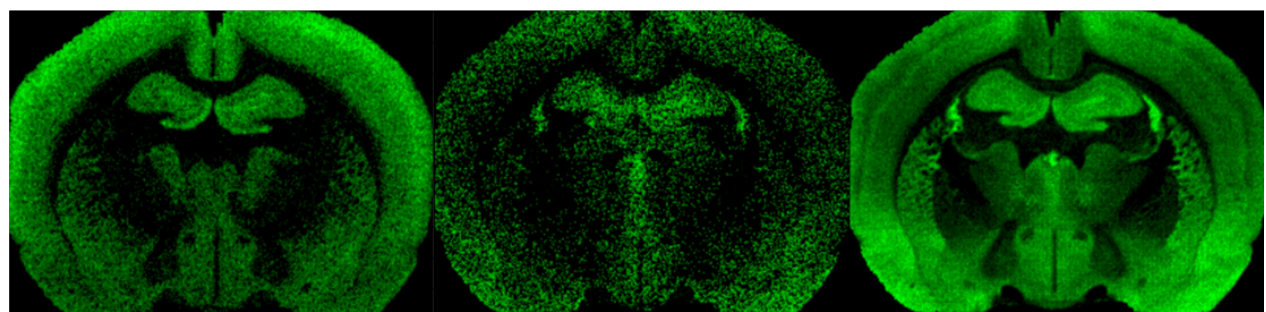
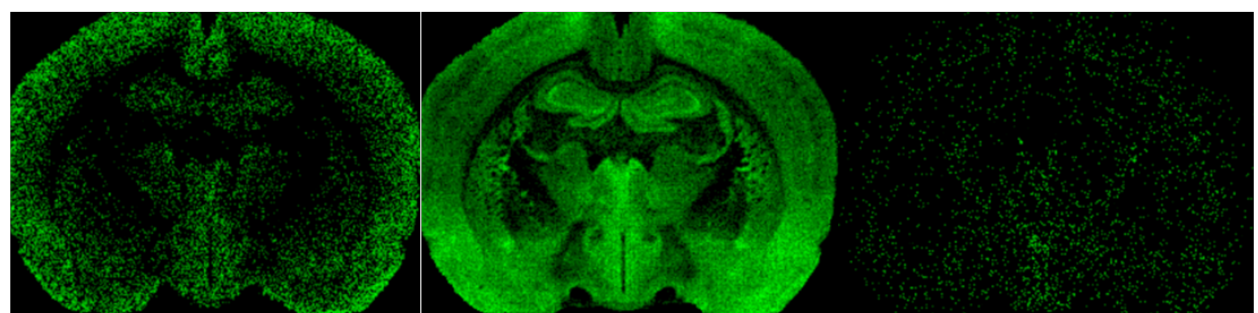
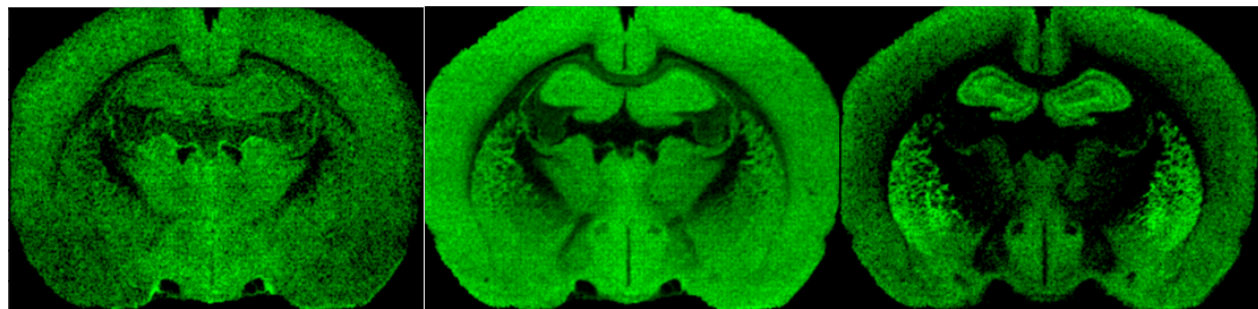


PE 36p:1
728.56

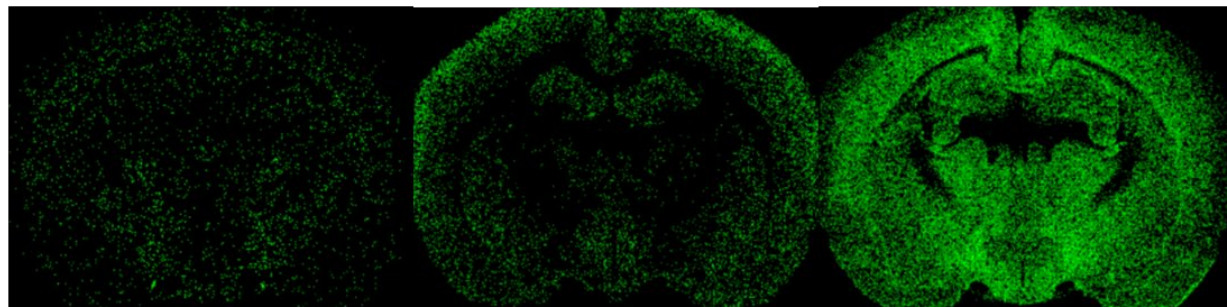
PE 36p:0
730.58

PE 36a:4
738.51

Phosphatidylethanol (PE)
Negative ion mode
(M-H)⁻



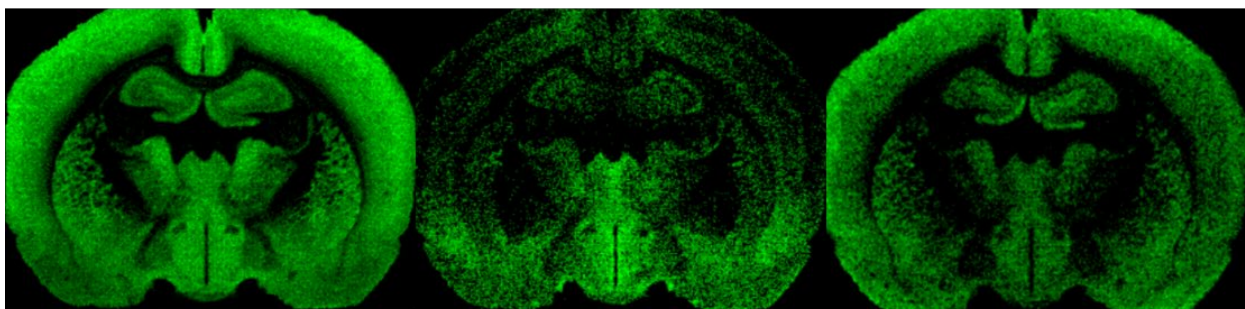
Phosphatidylethanol (PE)
Negative ion mode
(M-H)⁻



PE 38a:2
770.52

PE 40p:7
772.53

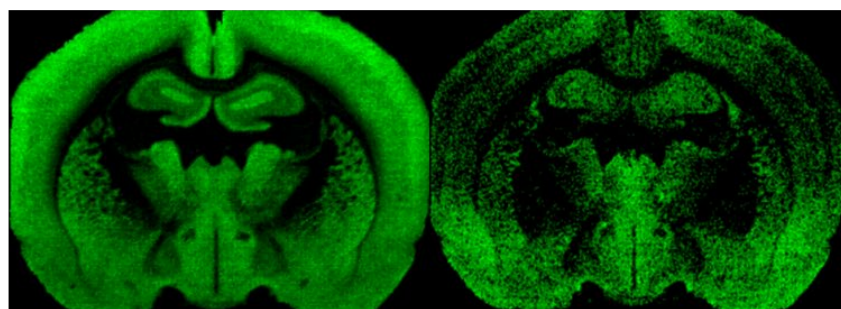
PE 38a:1
772.59



PE 40p:6
774.54

PE 40p:4
778.58

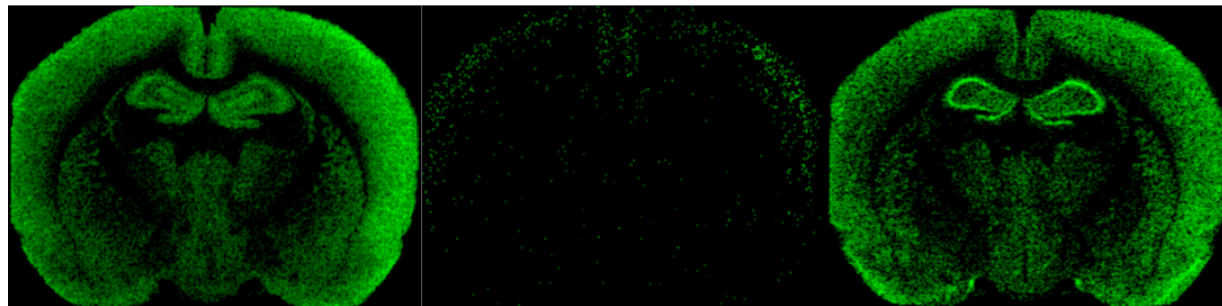
PE 40a:7
788.52



PE 40a:6
790.54

PE 40a:4
794.57

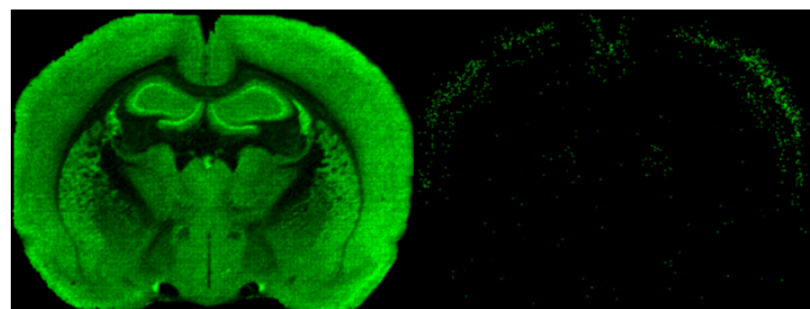
Phosphatidylinositol (PI)
Negative ion mode
(M-H)⁻



PI 36:4
857.52

PI 38:6
881.52

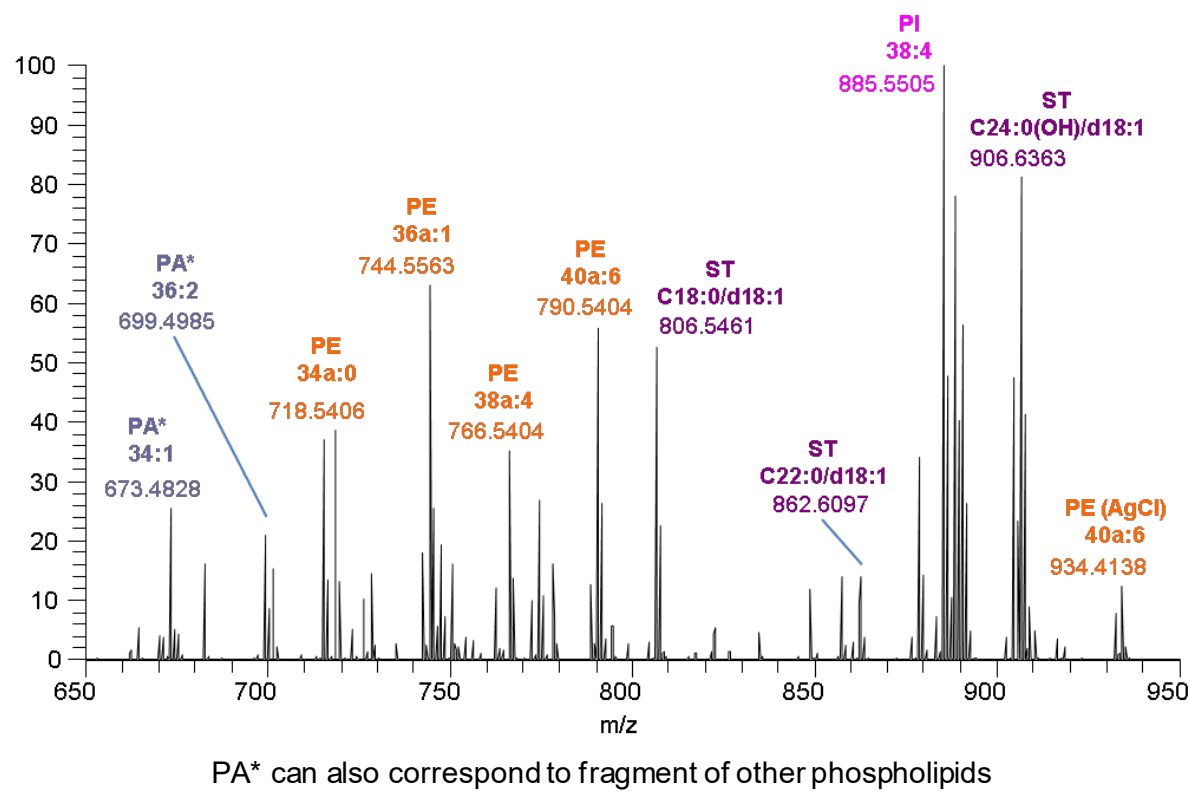
PI 38:5
883.53



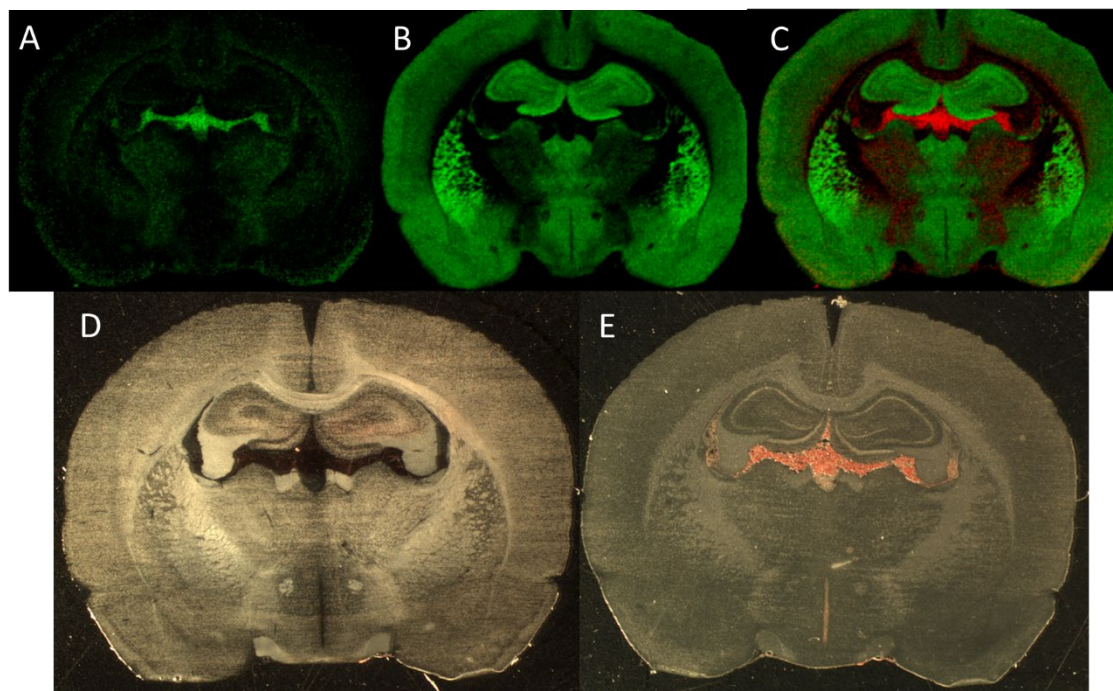
PI 38:4
885.55

PI 40:6
909.54

Supplementary figure 5: MALDI average mass spectrum from a serial rat section, acquired in negative ion mode on a MALDI-LTQ-Orbitrap-XL with silver nanoparticles matrices.



Supplementary figure 6: Distribution of ceramides by mass imaging of a rat at brain section level -2.0 mm re:Bregma in positive ion mode. Images were extracted for m/z (A) 756.5420 corresponding to Cer 20:0/d18:1+Ag, (B) 672.4479 corresponding to Cer 18:0/d18:1+Ag and (C) Combo plot of both ceramides Cer 20:0/d18:1+Ag (red) and Cer 18:0/d18:1+Ag (green). Microscope image (D) before and (E) after implantation



Supplementary figure 7: Distribution of ceramides by mass imaging at level -3.2 mm re:Bregma in positive ion mode in a rat brain section, resolution 100,000 at 400 u. Images were extracted for m/z (A) 644.4166 corresponding to Cer 16:0/d18:1+Ag, (B) 670.4323 Cer 18:1/d18:1+Ag (C) 672.4479 corresponding to Cer 18:0/d18:1+Ag and (D) 700.4792 corresponding to Cer 20:0/d18:1+Ag.

